

# Study on FRT compliance of VSC-HVDC connected offshore wind plants during AC faults including requirements for the negative sequence current control



Mario Ndreko<sup>a,\*</sup>, Marjan Popov<sup>a</sup>, Mart A.M.M. van der Meijden<sup>a,b</sup>

<sup>a</sup> Delft University of Technology, Faculty of EEMCS, Intelligent Electrical Power Grids, Delft, The Netherlands

<sup>b</sup> TenneT TSO B.V., Arnhem, The Netherlands

## ARTICLE INFO

### Article history:

Received 19 April 2016

Received in revised form 17 June 2016

Accepted 21 August 2016

Available online 29 August 2016

### Keywords:

VSC-HVDC

Negative sequence current control

FRT

Unbalanced faults

Offshore wind power grid connection

## ABSTRACT

In this paper three new control modules are introduced for offshore wind power plants with VSC-HVDC transmission. The goal is to enhance the Fault Ride Through (FRT) capability of the HVDC system and the connected offshore wind power plant during balanced and unbalanced AC faults. Firstly, a positive-sequence-voltage-dependent (PSVD) active current reduction control loop is introduced to the offshore wind turbines. The method enhances the performance of the offshore AC voltage drop FRT compliance strategy. Secondly, an adaptive current limiting control strategy which operates simultaneously on the positive and the negative sequence current is discussed. It enables negative sequence current injection, while at the same time respecting the maximum fault current capacity of the HVDC converter station. Finally, a state machine is proposed for the VSC-HVDC system and for the offshore wind turbines respectively. It coordinates the fault and the post-fault response during balanced as well as unbalanced faults, ensuring a smooth shift from the normal operating point towards the fault and the post-fault period. The test system consists of a two level VSC-HVDC link, rated at  $\pm 250$  kV, connecting an offshore wind power plant with 700 MW generation capacity. Simulation results with a detailed EMT type model in PSCAD/EMTDC environment are presented.

© 2016 Elsevier Ltd. All rights reserved.

## 1. Introduction

It is well known that voltage source AC/DC power converters suffer from double synchronous frequency ripples observed in the active power and the DC link voltage when they are exposed to unbalanced AC grid voltages. A variety of control techniques to mitigate this phenomenon have been proposed initially for low power converters [1–3] and later expanded to wind turbine applications [4,5]. Next to the design of such negative sequence current control schemes, their effect on the protection of AC transmission systems is stressed in [6,7] for AC connected wind power plants.

For VSC-HVDC applications, an analysis of negative sequence current control is presented in [8] for the particular case of embedded in the power system VSC-HVDC link. In [9], the unbalanced fault response of the offshore wind power plants with VSC-HVDC connection is investigated for the first time during offshore AC faults. The emphasis is placed on the double frequency harmonic mitigation and not on the power system protection needs. In addition,

it is not demonstrated how the VSC-HVDC system as well as the connected to it offshore wind turbines ensure that their over-current capacity is not violated during the combined positive and the negative sequence current injections. In that prospect, a step-wise adaptive positive and negative sequence current limiting control scheme is discussed in [10]. The method demonstrates satisfactory results, however, the over-current capacity of the HVDC station is over-sized compared to real system applications. In addition, the classical chopper based solution is used and not the state of the art voltage-drop Fault-Ride Through (FRT) strategy.

A variety of FRT strategies for offshore VSC-HVDC systems have been documented in the literature, using either offline simulations [11–15] or real time digital simulators (RTDS) [16]. In vast majority of these papers, the offshore island AC system is aggregated by an equivalent wind turbine model directly connected to the HVDC station, neglecting the potential effect of the offshore AC island grid. Furthermore, the voltage drop FRT strategy [13–16] is demonstrated for balanced faults using very simple control schemes at the offshore HVDC converter station and not the state of the art cascaded current-controller that manufacturers utilize today. Although, recently a lot of research effort is spent on the new gen-

\* Corresponding author.

E-mail address: [m.ndreko@tudelft.nl](mailto:m.ndreko@tudelft.nl) (M. Ndreko).

eration of HVDC transmission, the MMC-HVDC [17–21], yet a number of issues related to the two-level HVDC links need to be addressed.

This paper proposes an improved FRT control strategy which enables the offshore wind turbines to participate in the overall FRT compliance of the VSC-HVDC link during onshore AC grid faults. The method is based on an applied active current reduction to the offshore wind turbines. It is performed as a function of the imposed AC voltage drop by the offshore HVDC station. No communication links are used. For the special case of unbalanced onshore AC grid faults, a new adaptive current limiting control module is introduced at the onshore VSC-HVDC station. Furthermore, this adaptive current limiter is supported by a negative-sequence-voltage-dependent (NSVD) active current reduction module which enables a higher injection of the negative sequence current injection while respecting the over-current capacity of the HVDC station. The proposed controllers are tested for balanced as well as for unbalanced AC faults (namely for line-line faults) at the onshore and the offshore AC terminals where FRT compliance need to be demonstrated. For the case of the offshore AC collector grid faults, it is demonstrated that the application of the proposed FRT strategy does not jeopardize the fault detection ability in the island offshore grid. Finally, the FRT and post-FRT response is guided by state machines at the onshore VSC-HVDC station and at the offshore wind power plants respectively. Time domain simulations with detailed EMT type models in PSCAD/EMTDC are presented. The results of this paper can be used as reference for the grid code design and FRT compliance studies of offshore wind plants with VSC-HVDC connection.

## 2. Test system used

A 200 km HVDC link is used in this work, rated at  $\pm 250$  kV. It provides grid connection to a 700 MW offshore wind power plant. The grid side VSC-HVDC station (GSVSC) is interfaced to the infinite grid via a 30 km transmission line at 380 kV as it is presented in Fig. 1. The offshore AC island grid consists of two HVAC cables at the 150 kV voltage level. A pair of three-winding transformers are used to interface the 150 kV cables to the 33 kV feeders. Detailed models are used for the three winding transformers including their saturation effect. The HVAC cables offshore are represented with a pi-equivalent model with 7.5 km and 4.5 km length respectively. The group of the wind turbines which are connected per each feeder are aggregated to an equivalent full converter permanent magnet wind turbine model connected at the 33 kV terminal.

## 3. Model and control strategies of the onshore VSC-HVDC station

### 3.1. Dual synchronous reference frame control scheme

The so called dual synchronous reference frame (SRF) control scheme, is used at the onshore HVDC converter station in order to control simultaneously the positive and the negative sequence current [1]. A SRF-PLL is utilized both for the positive and for the negative sequence current control modules as presented in Fig. 2. Notch filters, tuned at the double synchronous frequency have been utilized. Fig. 2 presents the control system layout for the onshore converter HVDC station.

### 3.2. Positive sequence outer control loops

The positive sequence active current (d-axis current) of the onshore converter station is assigned to control the direct voltage of the HVDC link. The controller is mathematically given in time domain by:

$$i_{d+}^{ref} = k_{p,U_{dc}}(U_{dc}^{ref} - U_{dc}) + \int \left( \frac{U_{dc}^{ref} - U_{dc}}{T_{i,U_{dc}}} \right) dt. \quad (1)$$

where  $k_{p,U_{dc}}$  is the proportional gain,  $T_{i,U_{dc}}$  is the time constant of the PI regulator and  $U_{dc}$  the measured pole-to-pole direct voltage of the HVDC link. The reactive current control loop ( $i_q$ ) provides a continuous slow AC voltage support during the normal operation and a fast reactive short circuit current injection during AC system failures, as required by most of the grid code requirements [8]. The reactive current control loop is defined by (2), where  $k_{p,U_{ac}}$  is the proportional gain while  $T_{i,U_{ac}}$  is

$$i_{q+}^{ref} = k_{p,U_{ac}}(U_f^{ref} - U_f) + \int \left( \frac{U_f^{ref} - U_f}{T_{i,U_{ac}}} \right) dt + i_{q+}^{LVRT}. \quad (2)$$

the time constant of the AC voltage PI-regulator. Furthermore, the term  $i_{q+}^{LVRT}$  accounts for the positive sequence short circuit current injection of the onshore converter station during AC faults.

The fast reactive short-circuit current injection, implemented here by a proportional controller, is operating in parallel to the slow PI-based AC voltage controller. The mathematical description of the reactive short circuit current injection is given by (3).

$$i_{q+}^{LVRT} = \begin{cases} 0, & U_f \in [U_f^{DB-}, U_f^{DB+}] \\ k_1 (U_f^0 - U_f), & U_f \notin [U_f^{DB-}, U_f^{DB+}] \end{cases}. \quad (3)$$

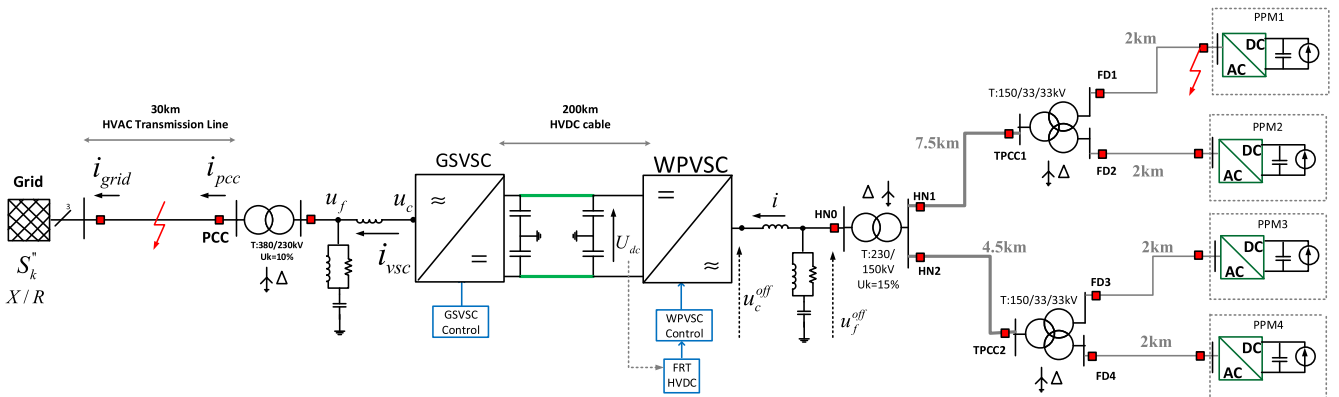
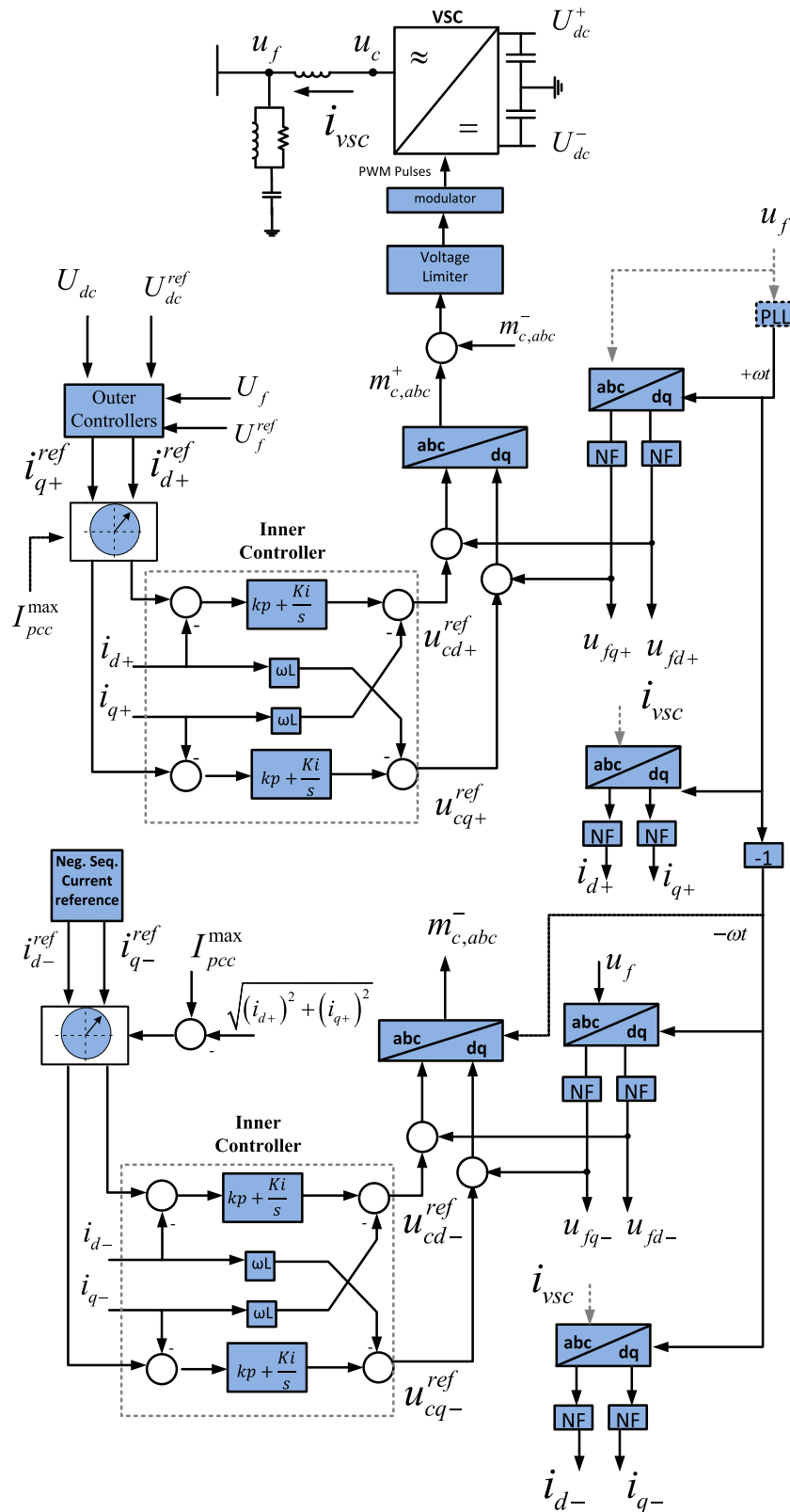


Fig. 1. The VSC-HVDC test system and the connected offshore wind power plant as it is used in this work.



In Eq. (3),  $k_1$  is the reactive current boosting gain (with typical values given in most grid codes between 2 and 10),  $U_f$  is the *rms* value of the filter voltage in per unit and  $U_f^{DB-}, U_f^{DB+}$  is the

lower and upper boundaries of the voltage dead-band which defines the voltage range that the reactive current injection is provided.

### 3.3. Coordinated fault and post-fault response of the VSC-HVDC onshore station

The FRT and post-FRT response of the onshore VSC-HVDC station during balanced and unbalanced AC faults is managed by the proposed state machine in Fig. 3. The input of the state machine is the positive sequence d-axis voltage component which is equal to the per unit value of the filter voltage. In the range between 0.9–1.1 p.u, the onshore HVDC converter station operates in normal condition (state S1). Once the voltage drops below the 0.9 p.u threshold, the converter operation shifts towards the LVRT state (S2). Reactive current limiting priority is selected as soon as the fault current capacity is reached. The converter supports the AC system voltage by injecting reactive current following Eq. (3). In the LVRT state (S2), the HVDC link direct voltage controller is set to the freeze mode and the duty of the HVDC link power balancing is explicitly managed by the FRT control scheme.

As soon as the voltage drops below the 0.5 p.u threshold, the converter enters the FRT mode (S3). In the FRT mode given that at least a reactive current boosting gain 2 is used (as it is commonly required by most grid codes), the positive sequence reactive current is taking all the fault current capacity, whilst the active current is reduced to zero. Hence, the choice of the 0.5 p.u voltage threshold is based on the fact that for AC voltages below 0.5 p.u, the reactive current injection leads to active current reduction even to zero by the positive sequence current limiter module. Consequently, post-fault when the voltage recovers, the converter shall move to state (S4), where a smooth ramping is ensured from the zero active current. For the case of voltage drops which are above 0.5 p.u, the converter returns from (S2) to (S1) without applying ramping. In the ramp-up state (S4), the active current is ramped following a predefined ramping rate  $R$  (pu/s). The selected ramping rate is a trade-off which affects the dynamic response of the AC system, as presented in [14]. The converter remains in the ramping state for a period  $T_r$  which ensures that the active current is ramped to the pre-fault level. Throughout the LVRT, FRT and ramp-up states of the HVDC link, the direct voltage controller and the slow AC voltage controller are blocked. This is done in order to avoid unwanted dynamics between the shift of states.

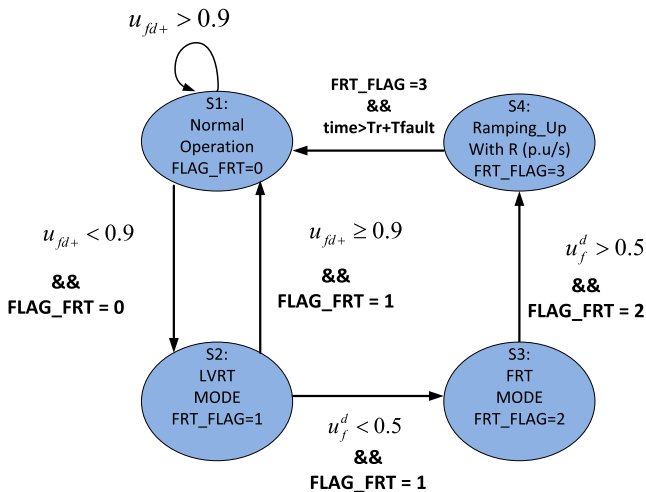


Fig. 3. State machine for the LVRT, FRT and post-FRT control logic which allows the implementation of the ramp-up function during the post-fault period ( $T_r$  is the ramping time calculated based on the ramping rate  $R$ , while  $T_{\text{fault}}$  is the time that the fault is applied).

### 3.4. Outer negative sequence current control loop

Two negative sequence current control strategies are tested for the VSC-HVDC system. First, the negative sequence current suppression and second, the negative sequence current injection. National level grid codes require for HVDC converters to be able to withstand negative sequence components during unbalanced line-to-line faults, without always making explicit which control strategy to be applied. This shall be decided based on the grid connection point needs per each connection. Normally, vendors apply negative sequence current suppression, as it ensures that the converter does not experience large unbalanced fault currents. The motivation for the negative sequence current injection is derived from the need to enhance the fault detection capability in combined AC-DC transmission systems, especially during the case of line-to-line AC faults [6,7].

#### 3.4.1. Suppression of the negative sequence current

The negative sequence current of the onshore converter station can be suppressed to the zero value during unbalanced voltages by applying the control references (4) and (5).

$$i_{d-}^{\text{ref}} = 0. \quad (4)$$

$$i_{q-}^{\text{ref}} = 0. \quad (5)$$

#### 3.4.2. Negative sequence current injection proportionally to the negative sequence voltage

The second approach which is studied in this paper is the injection of the negative sequence current proportionally to the negative sequence voltage. A proportional controller is used here, with proportional gain equal to  $k_2$ . During balanced conditions, the  $dq$ -voltage components in the negative SRF are zero while during unbalanced faults they increase. In this way the amplitude of the negative sequence voltage can be used in order to inject proportionally a negative sequence reactive current. The applied negative sequence current references are:

$$i_{d-}^{\text{ref}} = 0. \quad (6)$$

$$i_{q-}^{\text{ref}} = k_2 \sqrt{(u_{fd-})^2 + (u_{fq-})^2}. \quad (7)$$

### 3.5. Equivalent circuit of the onshore station during line-to-line faults

The equivalent circuit of the external 380 kV transmission line including the onshore VSC-HVDC converter station is presented in Fig. 4 for the line-to-line fault case. When the negative sequence current is suppressed (reflected with  $k_2 = 0$  in Fig. 4), the fault current contribution of the VSC station consists of the positive sequence current component  $I_1^{\text{VSC}}$ . This term includes the steady state value of the positive sequence current  $I_{1,0}^{\text{VSC}}$  and the positive sequence reactive current boosting term provided by Eq. (2). If during the unbalanced faults, the reactive current boosting gain ( $k_1$ ) is selected to be zero, the fault current injection of the VSC consists only of the steady state value current  $I_{1,0}^{\text{VSC}}$ . The latter depends on the operating point of the VSC. Some national level grid codes require for positive sequence reactive current injection ( $i_{q+}$ ) using Eq. (2) explicitly during balanced faults, while other grid codes does not differentiate the balanced from the unbalanced fault conditions.

In any of these two cases, the fault current contribution of the onshore VSC station during line-to-line faults can be increased by the injection of a negative sequence current. The latter choice



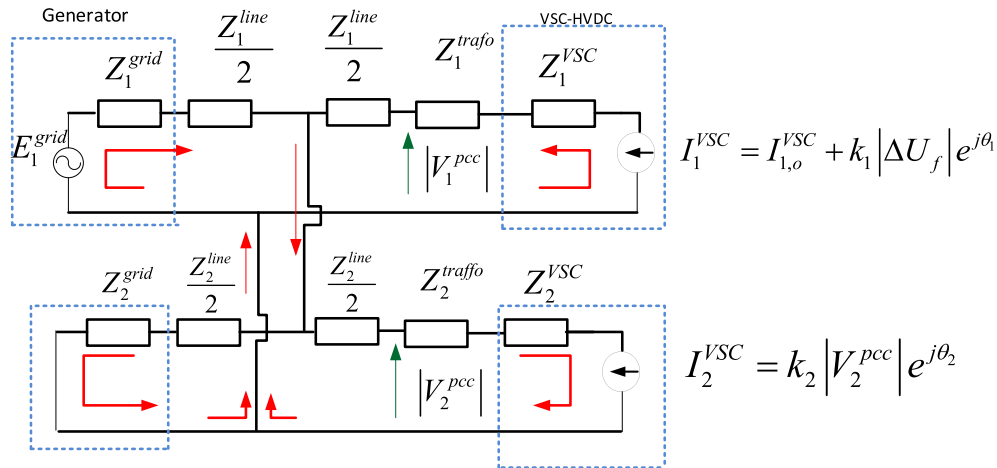


**Fig. 4.** Positive, negative and zero sequence equivalent circuits of the onshore converter station and the external grid for the line-line fault case study. The circuit helps to understand the EMT simulations presented below.

enables the converter to behave as a current source both in the positive as well as in the negative sequence circuit. Finally, the presence of negative sequence current in the AC transmission line terminals, enhances the unbalanced fault detection capability at the VSC side terminals of the AC line.

### 3.6. Adaptive positive and negative sequence current limiting module

The injection of combined positive and negative sequence currents during unbalanced faults shall respect the total fault current capability of the converter station. For that purpose, an adaptive negative sequence current limiting control module is proposed in this paper, as presented Fig. 2. The positive sequence maximum current limit is constant and it is equal to the over-current capacity of the converter (1.1 p.u). The negative sequence current limit ( $I_{\max 2}$ ) is adaptive. It uses as input signal the measured positive sequence current injection of the converter station. The module then calculates online the available overcurrent capacity left for the negative sequence current injection during unbalanced faults.

### 3.7. Negative sequence voltage dependent active current reduction for the GSVSC

In order to increase the negative sequence current share in the total onshore converter fault current injection, the positive sequence active current is reduced using the module in Fig. 5. We call it negative-sequence-voltage-dependent (NSVD) active current reduction as it is presented in Fig. 5. This control module is used especially in the case that the reactive positive sequence current injection is active during unbalanced faults. The negative-sequence voltage component is an incremental quantity, typically zero or very small under normal conditions, producing no pre-fault restraining bias. With purpose to avoid unnecessary active current reduction during switching transients, a dead-band of 0.3 p.u is also used. A quadratic function is applied in order to reduce the active current component. Hence, when the negative sequence current injection is selected as an option, the reduction of the positive sequence active current ( $i_{d+}$ ), enables the share of the current capacity by the positive and the negative sequence reactive currents. It is worth to note that if the grid code does not require for reactive positive sequence current injection during unbalanced faults, only the negative sequence current is injected following (Eqs. (6) and (7)).

## 4. Model and control strategies for the offshore VSC-HVDC station

The control scheme of the offshore VSC station is presented in Fig. 6. The main control objective is to provide a controlled AC voltage and frequency at the island offshore AC grid. This allows the PPL of the wind turbines to synchronise to the island voltage. A PLL at the offshore converter station is not needed during normal operation as the angle for the Park transformation is given directly from the frequency regulator as in Fig. 6. During the normal conditions at the offshore converter, the control modules ensure that the rated power is respected. As it can be seen in Fig. 6, the control approach uses an outer current control loop which sets the references of the inner current loop.

### 4.1. Frequency regulator

The main goal of the frequency regulator is to regulate the offshore AC island frequency. This is performed by providing the adequate phase angle to the oscillator block as presented in Fig. 6. It is important to stress that the control scheme used here is very similar to the power synchronization control loop as it is given in [16]. The difference of this paper approach lies on the fact that the frequency is regulated and not the active power.

### 4.2. Current controller reference

The equations which describe the calculation of the inner current control loop references are given in (8) and (9). The AC filter current is included in the control loop. The voltage references for the  $dq$ -axis are set to be one and zero respectively.

$$i_{cd}^{ref} = i_d - \omega C_f u_{fq} + k_{p1} (u_{fd}^{ref} - u_{fd}) + k_{i1} \int (u_{fd}^{ref} - u_{fd}) dt \quad (8)$$

$$i_{cq}^{ref} = i_q - \omega C_f u_{fd} + k_{p2} (u_{fq}^{ref} - u_{fq}) + k_{i2} \int (u_{fq}^{ref} - u_{fq}) dt \quad (9)$$

### 4.3. Current controller

The equations which describe the inner current controller are given in (10) and (11). The output of Eqs. (8) and (9) are used to define the internal  $dq$ -voltage of the converter station. The generated  $dq$ -reference voltages are limited by an upper threshold.

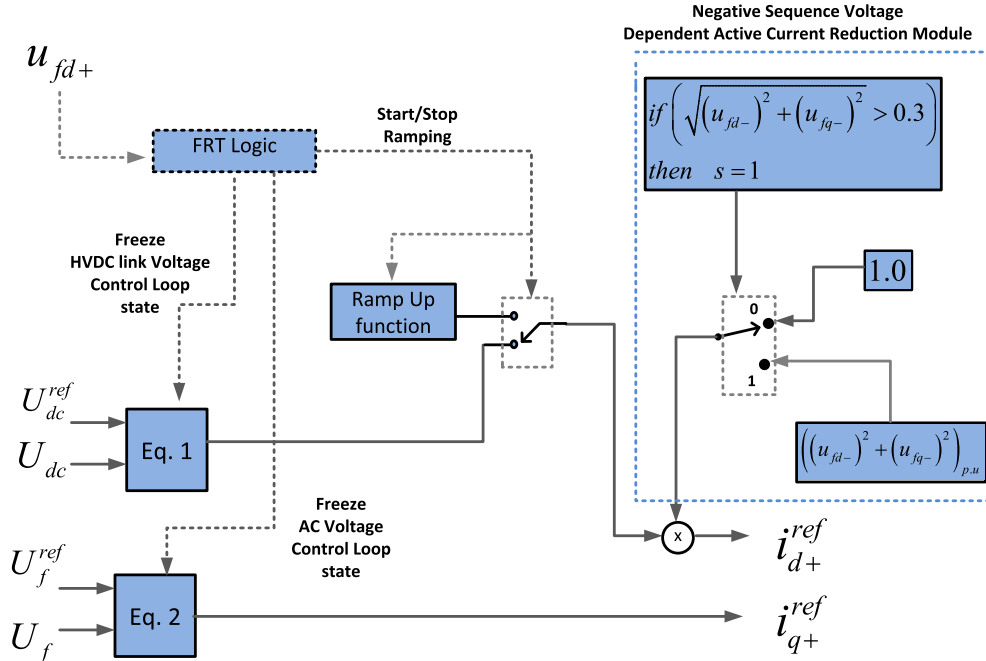


Fig. 5. Negative sequence voltage dependent active current reduction for the onshore VSC-HVDC station.

$$u_{c,ref}^d = i_{cd}R - \omega Li_{cq} - k_{p3}(\dot{i}_{cd}^{ref} - i_{cd}) - k_{i3} \int (\dot{i}_{cd}^{ref} - i_{cd}) dt \quad (10)$$

$$u_{c,ref}^d = i_{cq}R + \omega Li_{cd} - k_{p4}(\dot{i}_{cq}^{ref} - i_{cq}) - k_{i4} \int (\dot{i}_{cq}^{ref} - i_{cq}) dt \quad (11)$$

#### 4.4. Controlled AC voltage drop FRT strategy for the HVDC link

The controlled offshore AC voltage drop FRT compliance strategy is applied in this work as in Fig. 6 (termed here as “LVRT-HVDC” module). The voltage drop is applied proportionally to the HVDC link direct voltage, measured at the offshore DC terminal. Such a proportional controller is easier to be tuned, compared to other PI-based solutions. Furthermore, the “LVRT-HVDC” controller is designed such as the applied AC voltage does not drop below the 0.5 p.u. threshold, for the case of faults at the onshore AC terminal. This threshold is defined with the purpose to limit the electrical stresses imposed at the island grid. In order to achieve enhanced FRT compliance of the onshore converter station, an additional control loop is proposed here for the wind turbines. This control loop applies a positive-sequence-voltage-dependent (PSVD) active current reduction at the wind turbines as it will be discussed in following paragraph. The application of the AC voltage drop by the offshore station, along with the reduction of wind turbines active current enables the mitigation of the HVDC link over-voltage during FRT.

## 5. Model and control of the offshore wind power plants

### 5.1. Permanent magnet direct drive wind turbine model

The offshore wind power plant is assumed in this paper to be equipped with full converter interfaced permanent magnet wind turbine generators (commonly referred as type-4 in the IEC-61400 standard). The aggregation of the power plant is performed per each feeder at the 33 kV voltage level. An EMT type, average value model is utilized, presented in Fig. 7. The wind turbine inverter model is equipped with positive and negative sequence current

control loops. The permanent magnet generator and the generator side AC-DC rectifier are simply modelled here by a DC current injection. Since permanent magnet wind turbines utilize a DC chopper based FRT strategy, the electrical torque of the permanent magnet machine is completely decoupled from the AC grid voltage during AC grid faults. The latter ensures that the speed of the permanent magnet generator is not affected through the FRT process.

### 5.2. Positive sequence current control loops

The positive sequence current control loop of the equivalent wind turbine model enables decoupled active and reactive power control. In this work, the wind turbine inverter regulates the DC link voltage and the reactive power exchange with the AC island grid during normal operation. The reactive current control loop applies a PI regulator which controls the amplitude of the AC voltage at a given set point. In Fig. 7, it can be seen that the outer controller can be set to freeze state by the wind turbine FRT logic block which is presented below. Furthermore, a ramp-up linear function is used for ramping the active current during the post fault period of the wind turbine.

### 5.3. FRT logic for the wind PPM

The FRT and post-FRT response of the wind power plants is guided by the state machine of Fig. 8. Similar to the onshore HVDC station, the state machine is separated in four different operating states (S1–S4). The normal operating point state (S1) is defined for voltage values above 0.8 p.u. In this zone the wind turbine provides continuous AC voltage control to the island grid. As soon as the AC voltage at the wind turbine terminals drops below the 0.8 p.u. threshold, the wind turbine enters in state (S2).

Two could be the possible reasons for entering state (S2). First, an AC fault initiated at the onshore HVDC station, followed by the activation of the offshore VSC-HVDC station “LVRT-HVDC” module in Fig. 6. Second, a direct AC fault in the offshore AC island. In the state (S2), the wind turbine applies the positive-sequence-voltage-dependent (PSVD) active current reduction controller in Fig. 9. In

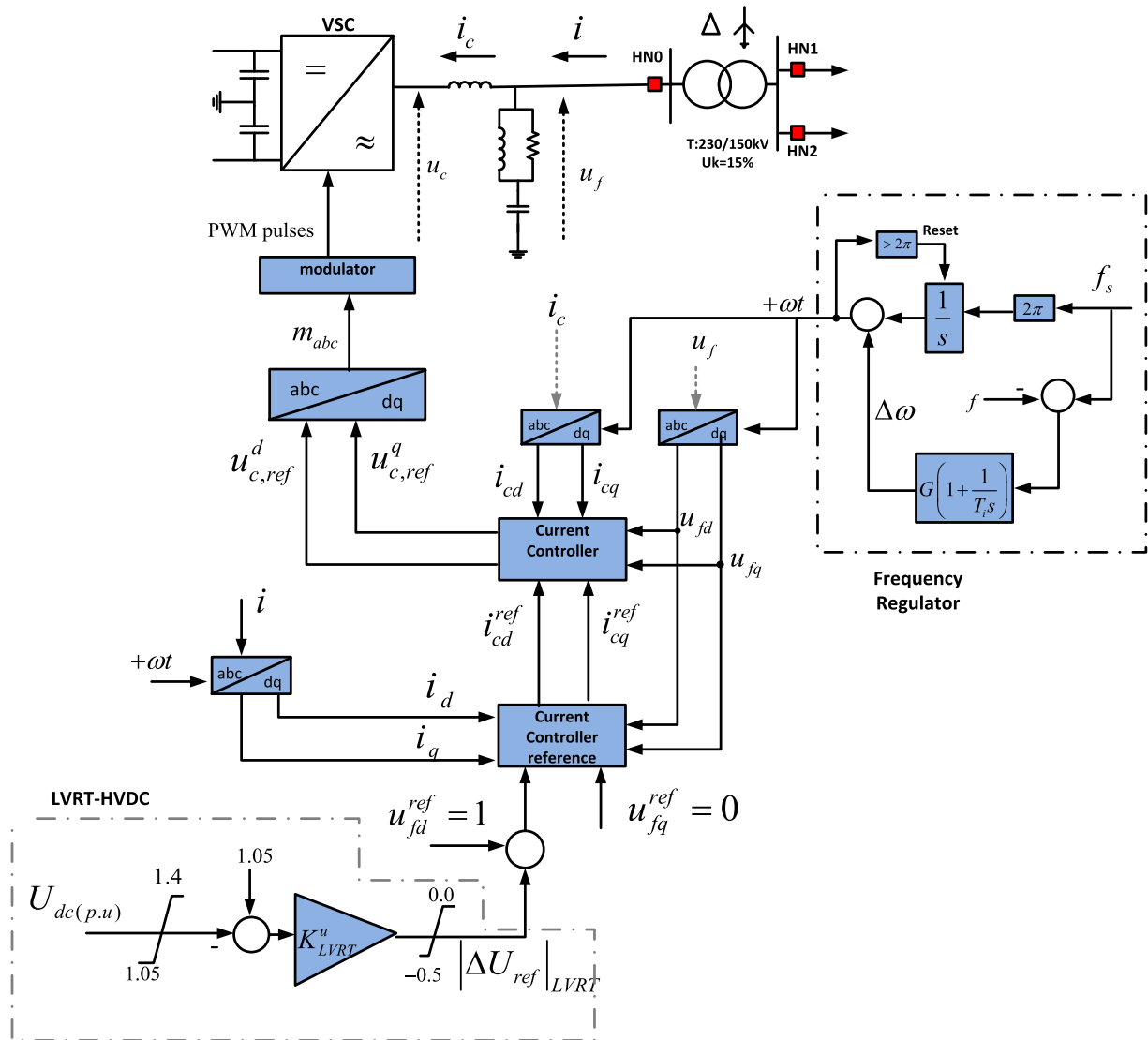


Fig. 6. Offshore converter station model and its control loops. In the figure with dashed lines is the “LVRT-HVDC” control loop and the frequency regulator control loop.

this way, the wind turbines reduce their active current providing FRT support to the HVDC link during onshore AC faults. The reduced active power is dissipated in the wind turbines choppers. Given that the offshore HVDC converter reduces its voltage only till 0.5 p.u (see Fig. 5), the wind turbines do not enter their FRT mode, state (S3). As soon as the onshore fault is cleared, the offshore voltage recovers and the wind turbines continues to operate returning to the normal operating state (S1). It is only during faults in the offshore island grid that the state (S3) is achieved. The slow AC voltage controller in the wind turbines is set to freeze mode for states (S2) to (S4).

It is recommended that a fast reactive current injection by the wind turbines shall be avoided in the state (S2) for two main reasons. First, it reduces the effectiveness of the active current reduction FRT control module (Fig. 7). Second, it creates high reactive power flows in the small island AC grid, which might jeopardize the stability of the offshore HVDC converter. It is important to mention that the voltage drop is artificially created by the offshore converter station. Hence, a very fast reactive current injection during the state (S2) without the presence of a physical fault, might lead to over-voltages and instability risks. Hence, the

0.3 p.u threshold between state (S2) and (S3) is selected in our case.

In the case of an AC fault in the offshore AC island, the wind turbine enters the state (S3). In (S3), a fast reactive current injection takes place proportionally to the residual voltage. In this state, since a fault occurs in the offshore AC island, the wind turbines support the voltage and provide reactive fault current for the protection schemes to detect and clear the fault. Finally, being in the state (S3), as soon as the wind turbines AC terminal voltage recovers, the wind turbines enter state (S4). Their active current is ramped-up, following a predefined ramp-up rate (p.u/s).

#### 5.4. Negative sequence current control loops

Modern wind turbines are equipped with negative sequence current control loops which enhances their dynamic performance during unbalanced AC faults. In this paper, a negative sequence current control loop as presented in Fig. 7 is applied. A variety of negative sequence current control strategies can be followed for the control of the negative sequence current during unbalanced grid faults. Similar to the onshore HVDC station case, two strate-

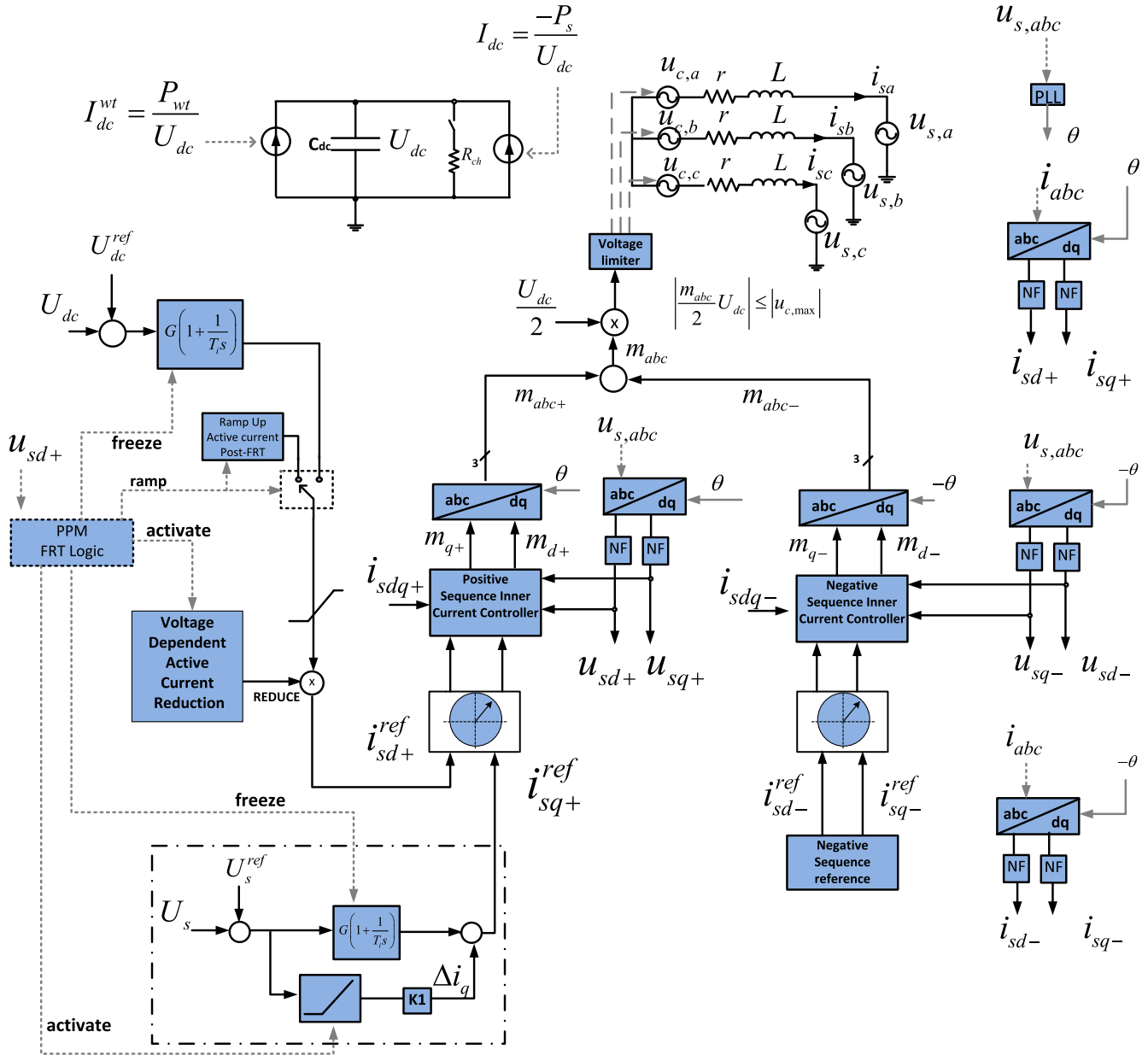


Fig. 7. Full converter interfaced wind turbine model and its positive and negative sequence current control loops.

gies are tested here for offshore AC grid unbalanced faults. The first strategy applies negative sequence current suppression [2] and the second strategy negative sequence current injection [6,7] proportionally to the negative sequence offshore voltage.

## 6. Simulation results and analysis

The proposed control modules in this paper are first evaluated for onshore AC grid faults. The response of the enhanced FRT control strategy and the negative sequence current control loops are demonstrated for balanced and unbalanced faults. Furthermore, unbalanced AC grid faults at the offshore AC terminals are presented in order to prove that the proposed FRT strategy does not affect negatively the response of the offshore island grid. The studied cases are namely:

- Three phase fault at the mid of the 380 kV transmission line onshore.

- Line-to-line fault at the mid of the 380 kV transmission line onshore.
- Line-to-line fault at the 33 kV terminals of the PPM1 aggregate model.

### 6.1. Three phase fault at the onshore transmission line – FRT demonstration

A 250 ms self-cleared three-phase-to-ground fault is applied at the mid-point of the 380 kV-HVAC transmission line. The onshore HVDC converter station provides a fast positive sequence reactive ( $i_{q+}$ ) current injection, utilizing a reactive current boosting gain  $k_1$  equal to 2. The voltage-drop FRT strategy, presented in Fig. 6 is applied. The onshore converter station utilizes its maximum fault current capacity as positive sequence reactive current ( $i_{q+}$ ) injection during the fault period, which leads to the reduction of the active current ( $i_{d+}$ ) to zero. During the post-fault period, the

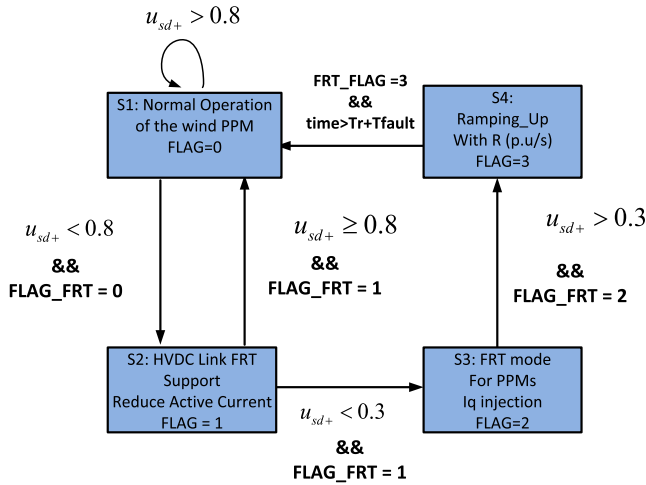


Fig. 8. State machine which guides the FRT control logic of the offshore wind turbines.

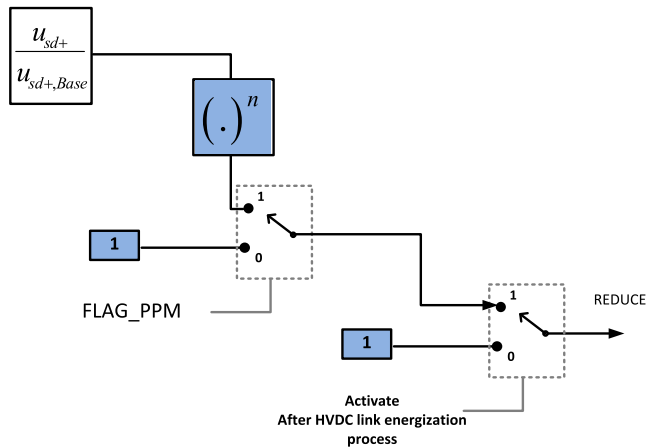


Fig. 9. Positive-sequence-voltage-dependent (PSVD) active current reduction module for the offshore wind turbines with VSC-HVDC connection.

active current is ramped up following a pre-selected ramping rate as presented in Figs. 10 and 11 (defined as in the state S4).

As it can be seen in Fig. 10, the ramping of the active current delays the direct voltage ( $U_{dc}$ ) recovery to the pre-fault steady state value. Furthermore, it increases the duration of the imposed offshore island voltage drop beyond the fault clearing time, as it can be seen in Fig. 12. Observing the negative sequence  $dq$ -currents in Fig. 11, it can be seen, that during the FRT period, the negative sequence current control loop does not affect the positive sequence current injection except the observed oscillations at the time that the fault is applied and cleared. The cause of these oscillations is the dynamic response of the notch filters. Moreover, the response of the dynamically-adaptive negative sequence current limiter ( $I_{max2}$ ) in Fig. 11.

In addition, the “LVRT-HVDC” controller (in Fig. 5) reduces the d-axis voltage component of the offshore HVDC converter terminal, while the q-axis component is controlled to zero. In this way the instantaneous voltage at the offshore VSC-HVDC station terminal is reduced as in Fig. 12. Furthermore, a positive sequence active current reduction is performed by the offshore wind power plants, applying the controllers of Fig. 9. During the LVRT period, no reactive current injection is provided from the wind turbines to the island grid as the wind turbines operate in the state S2. Fig. 13 pre-

sents the response of the active and reactive current in the wind turbine model which represents the dynamic response of PPM1.

It is presented that the proposed coordinated FRT strategy is capable to ensure FRT compliance, involving the participation of the offshore wind turbines in the process. Although a quadratic function ( $n = 2$  in Fig. 9) is used in this case for the active current reduction, a cubic or higher order function can be chosen as well to adjust the accepted over-voltage in the HVDC link.

## 6.2. Line-to-line fault at the onshore VSC-HVDC station

Next to the three-phase balanced fault simulations, a line-to-line fault case in the AC transmission system is studied. Five control options are discussed here. In the first, a negative sequence current suppression is applied ( $k_2 = 0$ , Fig. 4) while the positive sequence reactive current boosting is not active ( $k_1 = 0$ , Fig. 4). In the second case, we activate the positive sequence reactive current boosting ( $k_1 = 2$ , Fig. 4) similar to the balanced fault case, while the negative sequence current is suppressed ( $k_2 = 0$  in Fig. 4). In the third case, both positive and negative sequence current injections are provided ( $k_1 = k_2 = 2$ ). The bottlenecks of this option are stressed. As a solution, the response of the proposed negative-sequence-voltage-dependent (NSVD) active current reduction control module at the onshore converter station is presented in case 4. Finally, the application of the NSVD loop for the case without positive sequence reactive current injection is illustrated in case 5 ( $k_1 = 0$ ).

### 6.2.1. Case 1: $k_1 = 0$ and $k_2 = 0$

Fig. 14 presents the simulation results for a 250 ms self-cleared line-to-line fault at the mid-point of the 380 kV transmission line. As it can be seen, the negative sequence  $dq$ -current components ( $i_{dq-}$ ) are suppressed to zero while, the positive sequence  $dq$ -currents ( $i_{dq+}$ ) are kept constant during the fault period given that the active and reactive current control loops are set to freeze state. Fig. 14 presents the  $dq$ -voltages at the offshore HVDC station and the direct voltage of the HVDC link during the FRT period. As it can be seen, during the unbalanced fault period, the FRT process is activated in the same way as for the balanced faults. Observing the instantaneous value of the current at the PPC point, it can be seen that the fault current injection of the VSC is equal to the steady-state value current. It consists mainly of the positive sequence current component ( $I_1$ ), as in Fig. 15. The negative sequence current is suppressed while there is no zero sequence current in the external grid during line-to-line faults.

Observing the fault currents (positive and negative sequence) at the infinite grid terminals of the 380 kV transmission line in Fig. 15, it mainly consists of a high negative sequence component ( $I_2$ ) which is provided by the infinite grid.

### 6.2.2. Case 2: $k_1 = 2$ and $k_2 = 0$

The next option is to inject a positive sequence reactive current ( $i_{q+}$ ), while suppressing the negative sequence current of the onshore HVDC station ( $k_2 = 0$ ). The positive sequence reactive current is provided proportionally to the  $rms$  value of the line-line voltage measured at the filter of the VSC, in a similar way as performed for balanced faults utilizing a gain ( $k_1 = 2$ ). The controller (2) is applied. The simulations result are provided in Figs. 16 and 17.

Based on these results, it is observed that the positive sequence voltage support is not significant compared to the case (i). In that frame, the reactive positive sequence current injection does not provide significant benefits, at least for unbalanced faults.



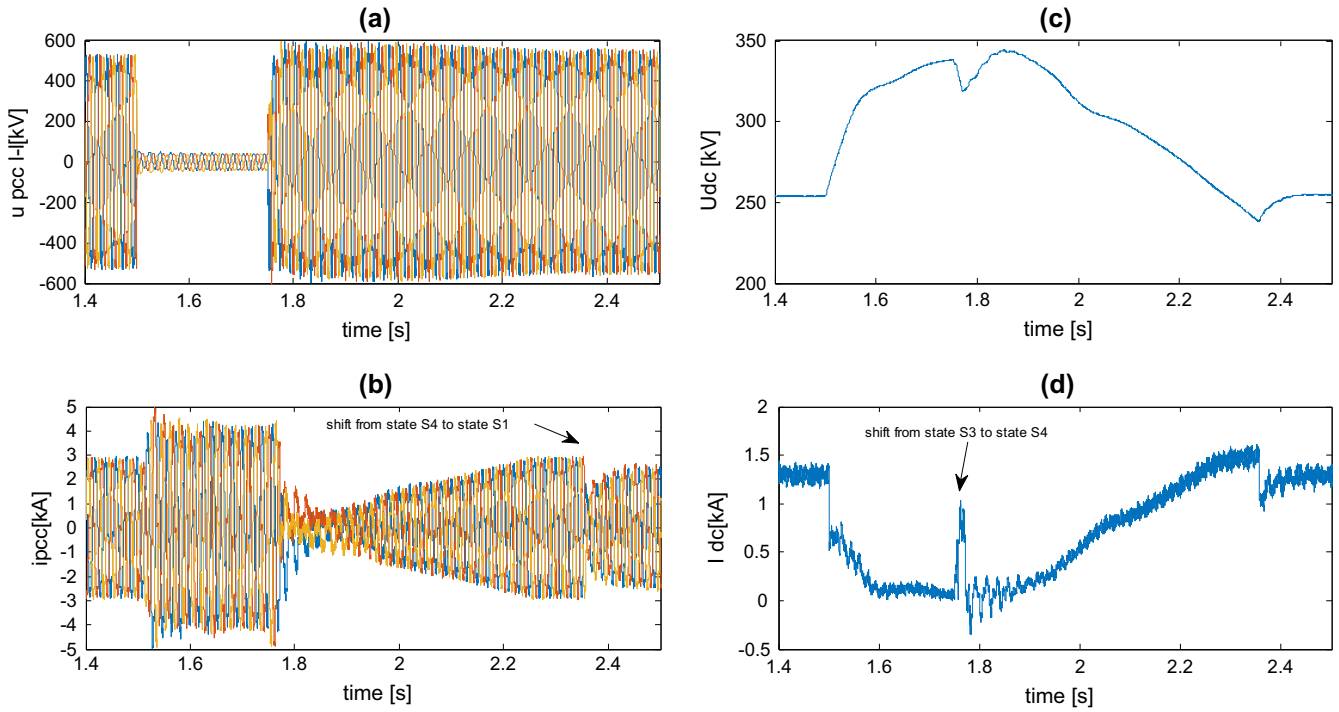


**Fig. 10.** (a) Instantaneous voltage, (b) instantaneous current at the onshore VSC-HVDC station, (c) offshore terminal direct voltage, (d) HVDC link direct current for the case of balanced three phase fault.

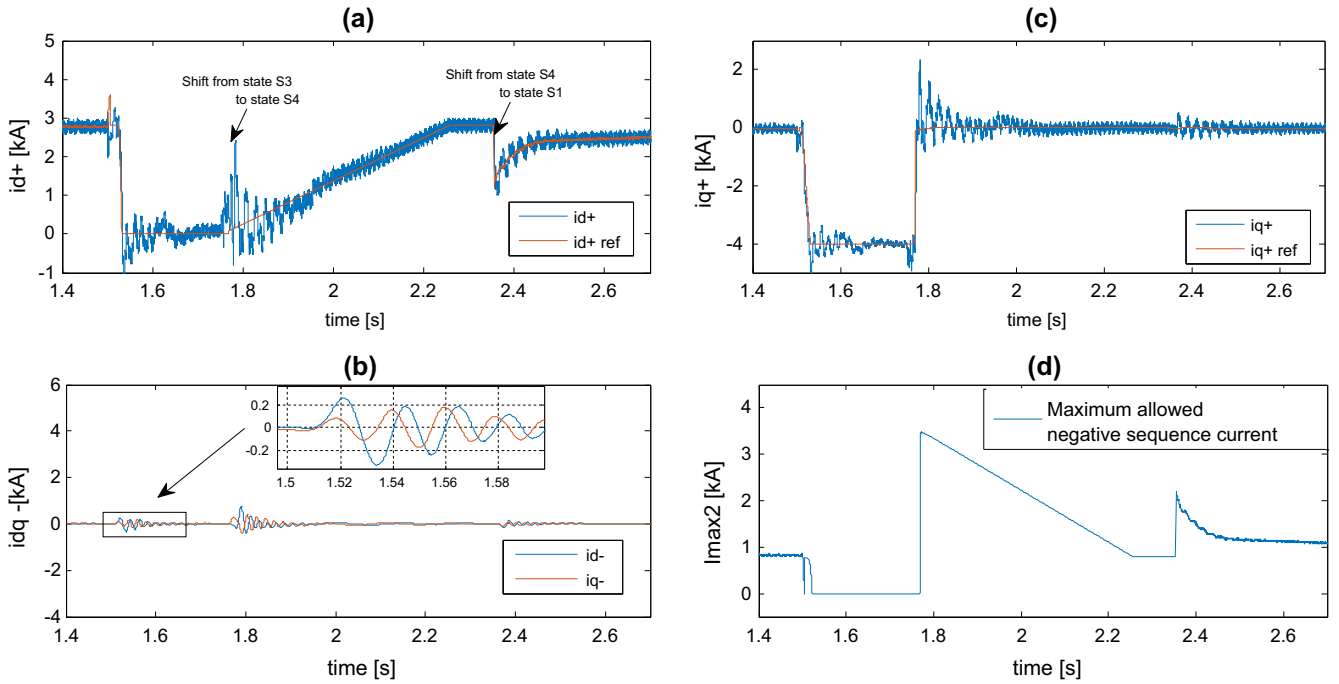


**Fig. 11.** (a) Positive sequence active current, (b) negative sequence dq-currents, (c) positive sequence reactive current, (d) maximum allowed negative sequence current given by the adaptive negative sequence current limiter.

### 6.2.3. Case 3: $k_1 = 2$ and $k_2 = 2$

With purpose to increase the negative sequence fault current injection by the onshore HVDC station, we utilize a combined positive and negative sequence current injection. The negative sequence current is injected during the unbalanced fault period proportionally to the negative sequence voltage following Eqs.

(6) and (7). However, this negative sequence current injection is bounded by the limited fault current capacity of the HVDC station.

One such case is simulated and presented in Fig. 18. Due to the limited over-current capacity, the HVDC station cannot provide the negative sequence current next to the positive sequence current. As it can be seen in Fig. 18, the maximum allowed negative

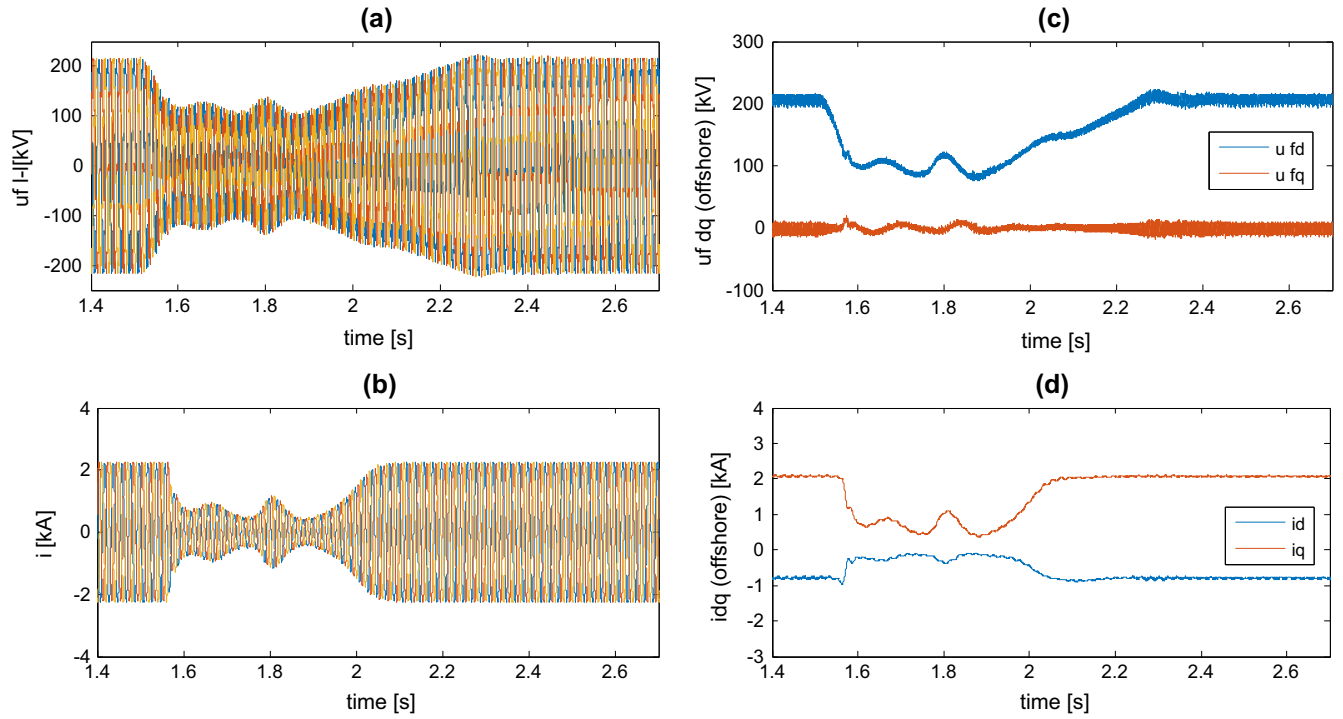


**Fig. 12.** Response of the wind plant side HVDC station during balanced fault at the onshore HVDC converter AC terminals. (a) Instantaneous voltage at the offshore filter, (b) instantaneous current at HNO breaker, (c) dq-voltages of the offshore converter station, (d) dq-currents of the offshore converter station.

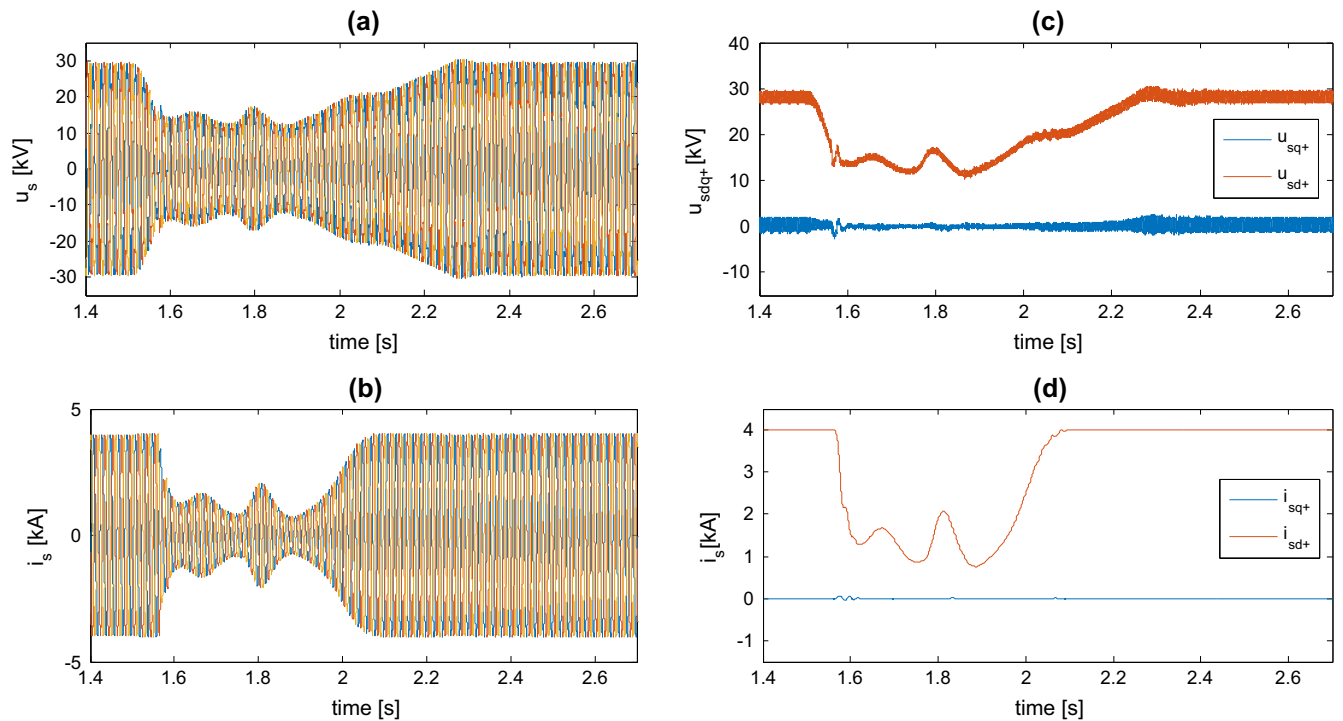


**Fig. 13.** Response of the offshore wind PPM1 after the reduction of the AC island grid voltage triggered by a fault in the onshore converter station terminals.

sequence current injection,  $I_{\max 2}$ , reaches the zero value during the fault period, leaving no available fault current space. Hence, a negative sequence current injection by the onshore converter station cannot be achieved unless the positive sequence current (either the active or the reactive current component) is reduced. The latter

justifies the need for the proposed control module of Fig. 5. By increasing the negative sequence current injection at the PCC side, an adequate fault detection method can be designed. Furthermore, the VSC behaves in similar way as the conventional generation units, enabling next to the positive, negative sequence current flow.

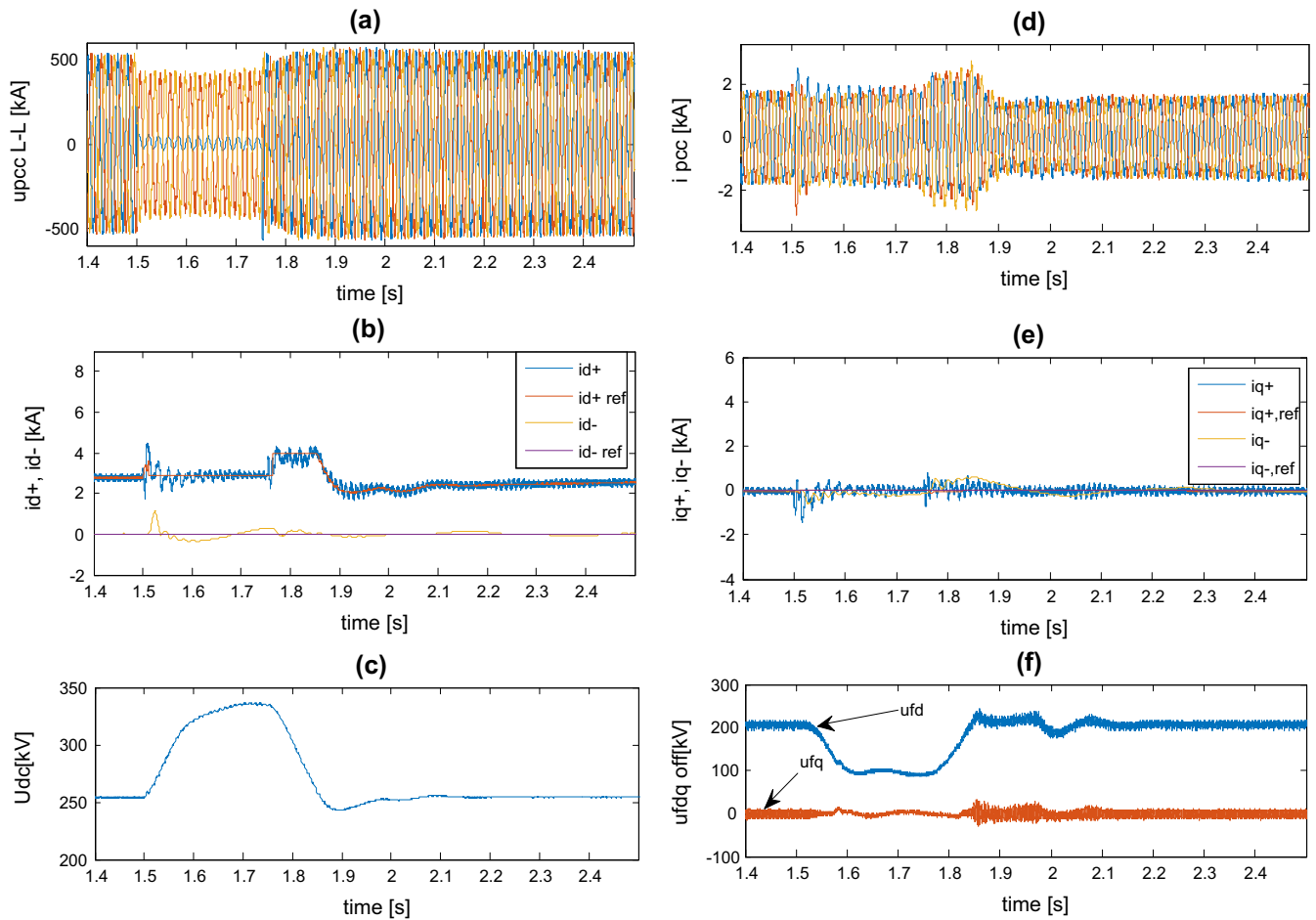


**Fig. 14.** Response of the VSC-HVDC link during a line-to-line fault at the onshore 380 kV transmission system (Case 1). (a) The instantaneous value of the onshore PCC voltage, (b) the active positive and negative sequence d-axis current, (c) the HVDC link direct voltage (d) the instantaneous current at the onshore HVDC station, (e) the positive and negative sequence reactive currents ( $i_q$ ) of the onshore station and (f) the dq-voltage of the offshore converter station.

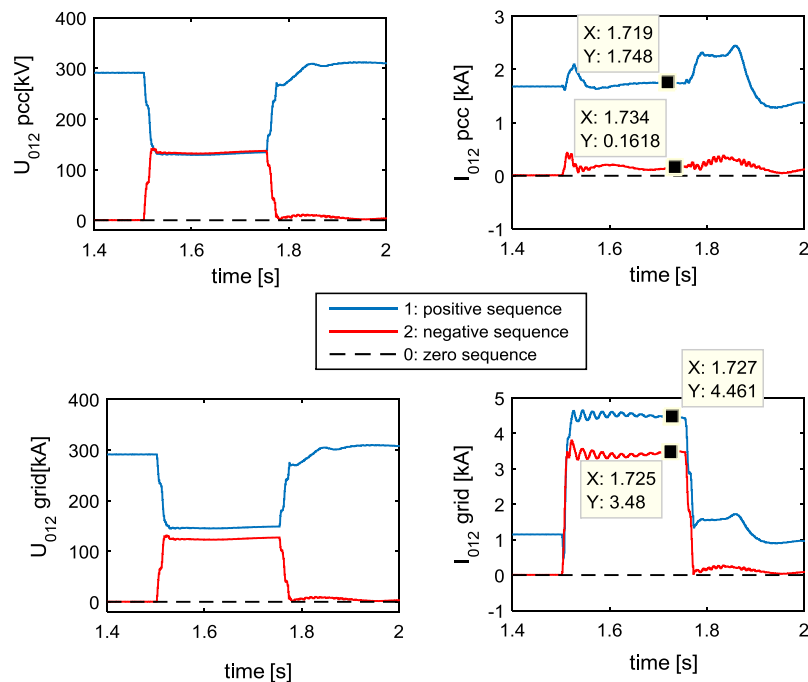


**Fig. 15.** Response of sequence components of the external AC grid voltages and currents (case 1). These plots relate to the sequence circuit of the external AC grid for the line-to-line fault case.

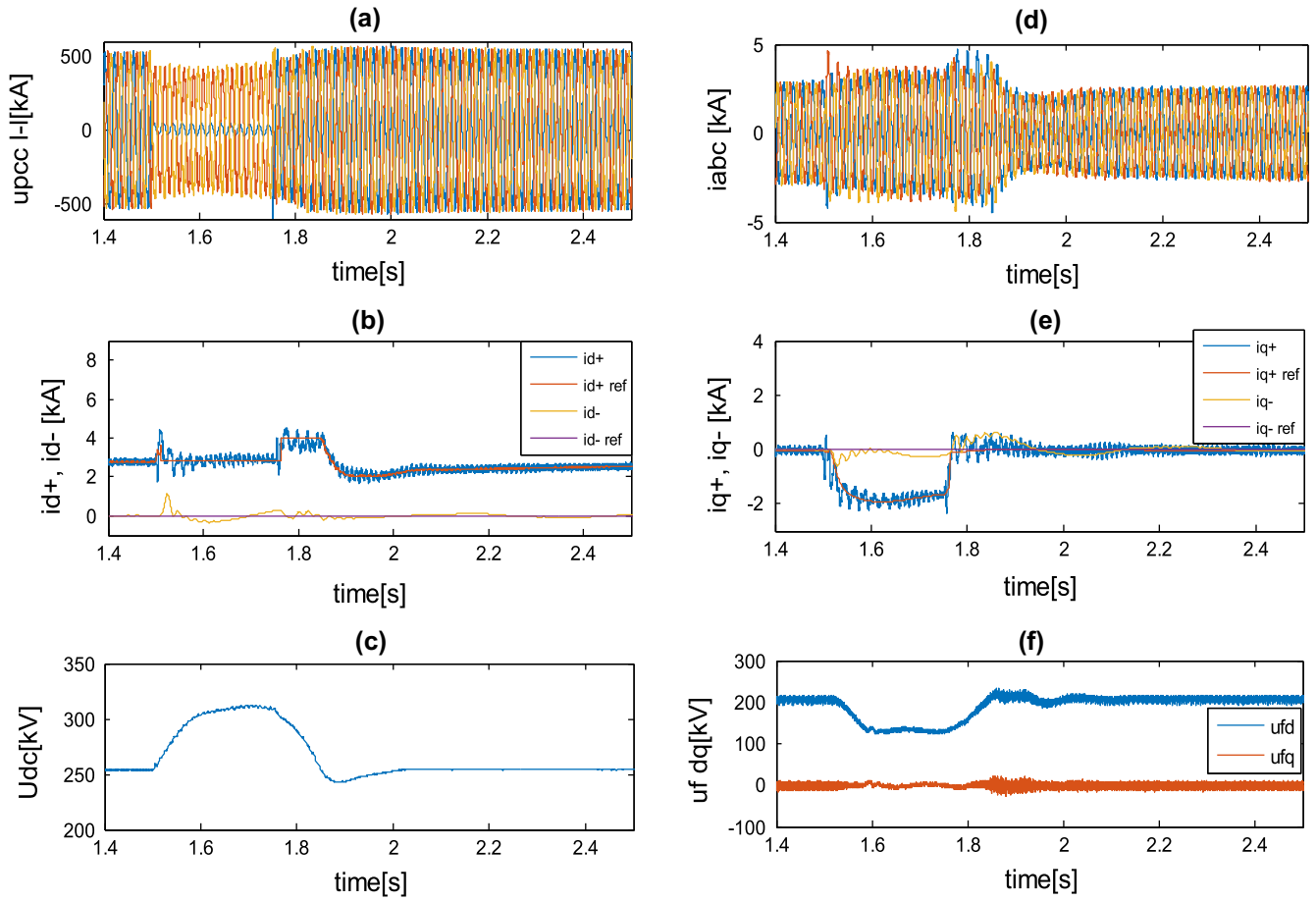


**Fig. 16.** Response of the VSC-HVDC link during a line-to-line fault at the onshore 380 kV transmission system (case 2). The palette shows from top to bottom the instantaneous value of the voltage and the current at the onshore HVDC station, the positive and negative sequence dq-currents of the onshore station, the HVDC line voltage and the dq-voltage of the offshore converter station.

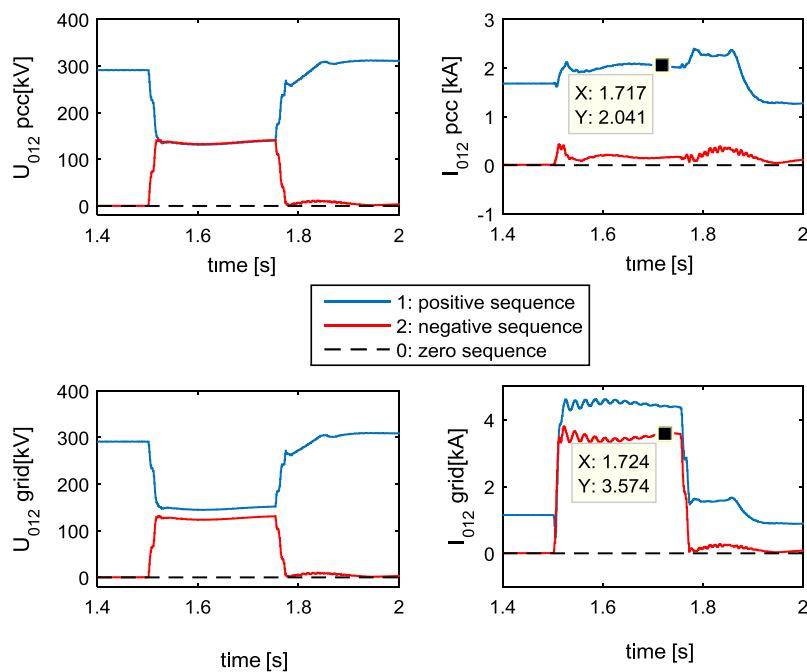


**Fig. 17.** Response of sequence components of the external AC grid voltages and currents for case 2.

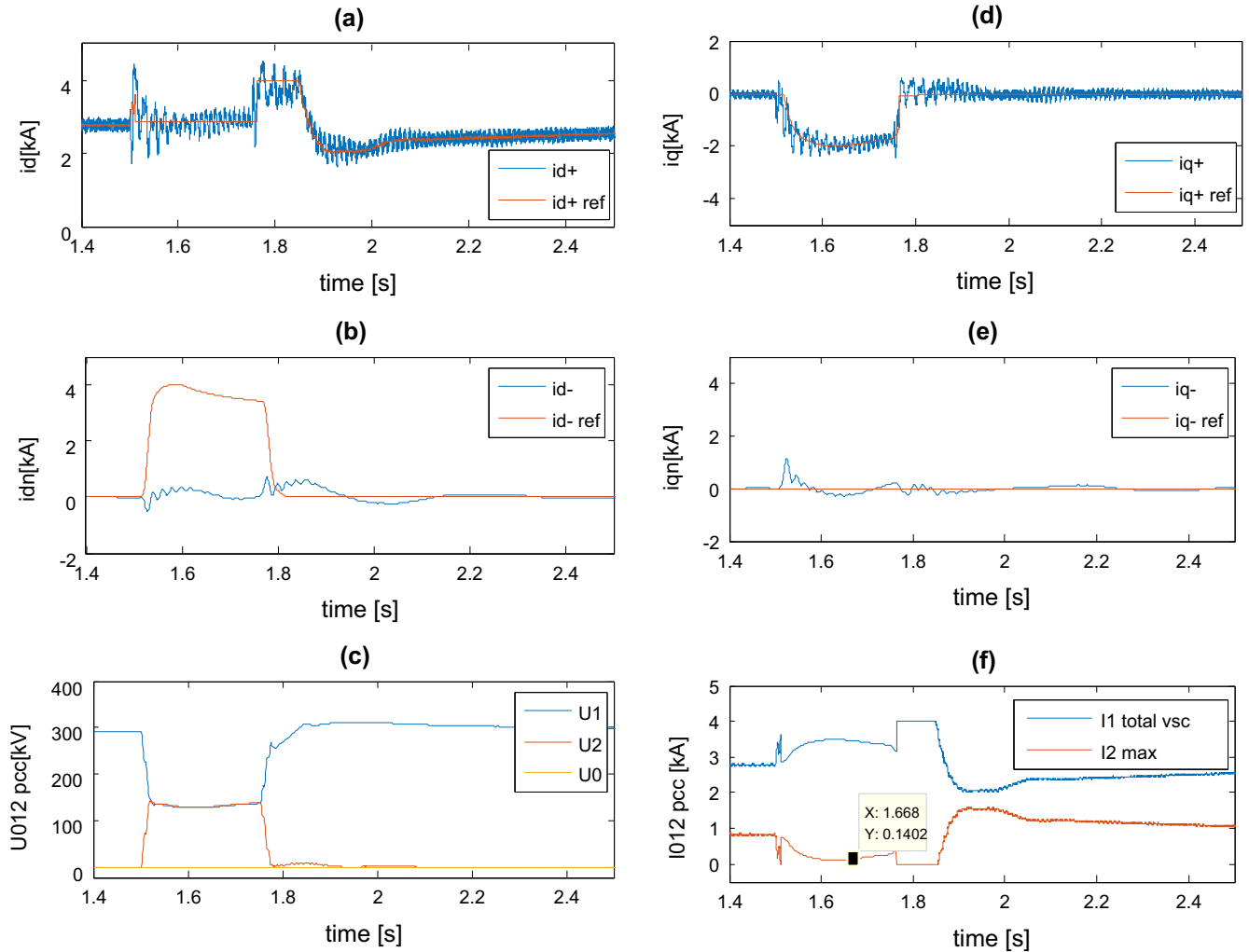


**Fig. 18.** Response of the GSVSC during balanced fault for case 3. (a) Positive sequence active current, (b) negative sequence reactive current, (c) sequence voltages at the PCC, (d) reactive positive sequence current, (e) negative sequence reactive current, (f) total current and negative sequence dynamic maximum current limiter.

#### 6.2.4. Case 4: $k_1 = 2$ and $k_2 = 2$ with negative-sequence-voltage-dependent active current reduction

In this paragraph, the active current reduction based on the negative sequence voltage is presented. Figs. 19 and 20, show the response of the system for the same disturbance. As it can be seen, the reduction of active current as a function of the negative sequence voltage gives additional space for the negative sequence current to be injected into the grid.

It is worth to observe that the injection of the negative sequence current gives rise to double frequency oscillations in the measured positive sequence dq-current ( $i_{dq+}$ ). The latter occur due to the coupling effect between the positive and the negative sequence dq-frames [2]. However, since the active current is reduced to zero, the imposed active power oscillations have small margin around the zero value.

#### 6.2.5. Case 5: $k_1 = 0$ and $k_2 = 2$ with negative-sequence-voltage-dependent active current reduction

Finally, when positive sequence reactive current boosting is not requested by the TSO during unbalanced faults ( $k_1 = 0$  in Fig. 4), the application of the NSVD loop in Fig. 5 enables the utilization of the VSC current capacity as negative sequence reactive current. The gain  $k_2$  is a control variable which defines the amount of the negative sequence current injection. Fig. 21 presents such a case study

for completeness. As it can be seen, the negative sequence current measured at the PCC is in the same range as at the infinite grid case.

### 6.3. Unbalanced faults at the 33 kV wind turbine terminal

In this paragraph, the response of the VSC-HVDC link is assessed for faults applied at the 33 kV offshore collector grid terminals. Only unbalanced faults will be presented due to space limitations. The goal of this paragraph is to prove that the applied active current reduction at the wind turbines as part of the FRT strategy does not affect the fault detection ability at the offshore AC island.

#### 6.3.1. Case1: Line-to-line fault at the 33 kV with negative sequence current suppression and $k_1 = 0$

A line-to-line fault is applied at the 33 kV terminal of the power plant module 1 (PPM1 in Fig. 1). The PPM1 utilizes the negative sequence current suppression control strategy. Furthermore, it is assumed that no positive sequence reactive current is injected into the island grid from the offshore PPMs during the fault period. Fig. 22 presents the instantaneous value of the voltage and the current at the PPM1 AC terminals, at the FD1 point and at the offshore HVDC converter station terminals (point of HN0). The dq-components of the voltage and the currents of the PPM1 can be



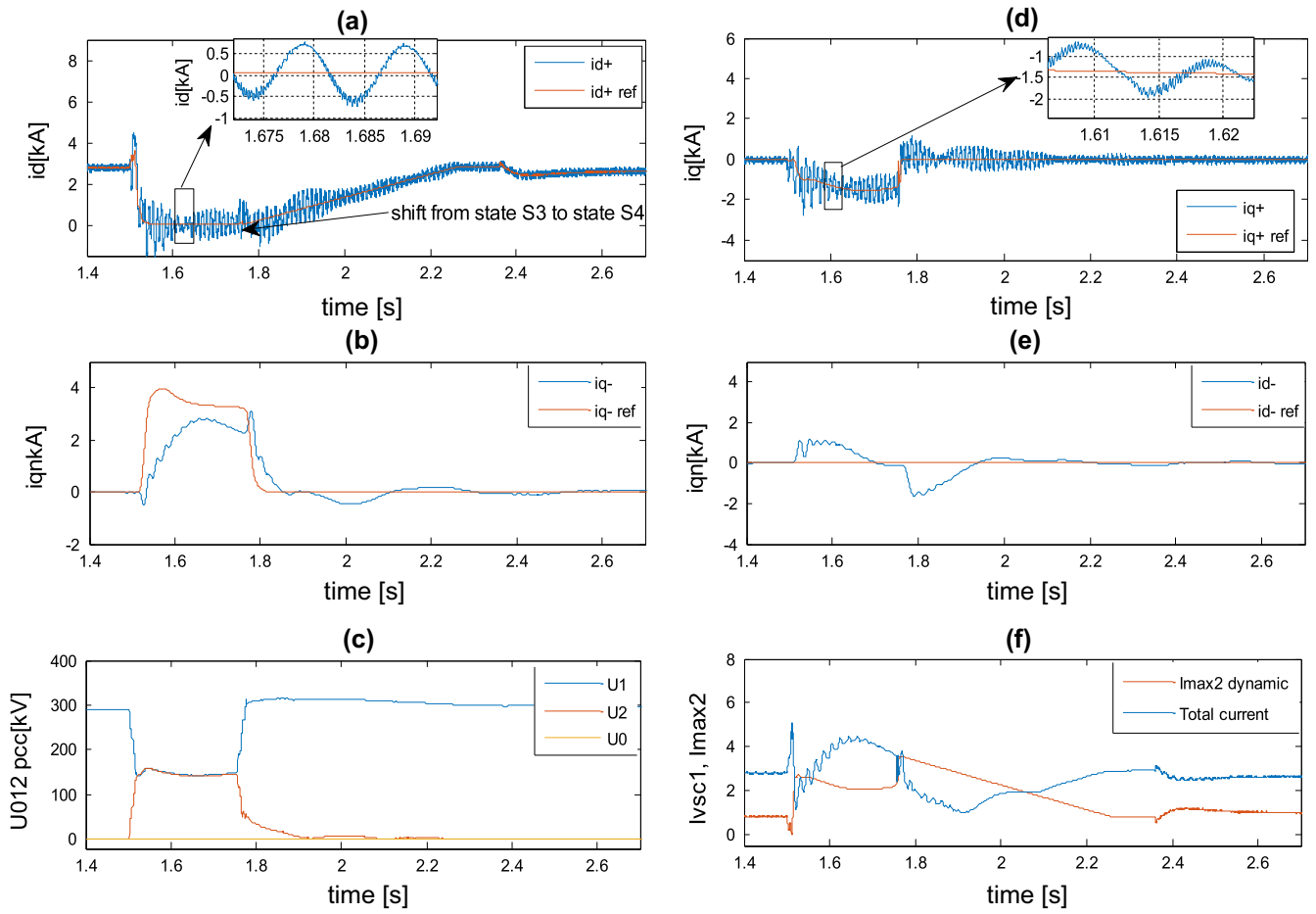


**Fig. 19.** Response of the GSVSC during balanced fault for case 4. (a) Positive sequence active current, (b) negative sequence reactive current, (c) sequence voltages at the PCC, (d) reactive positive sequence current, (e) negative sequence reactive current, (f) total current and negative sequence dynamic maximum current limiter.

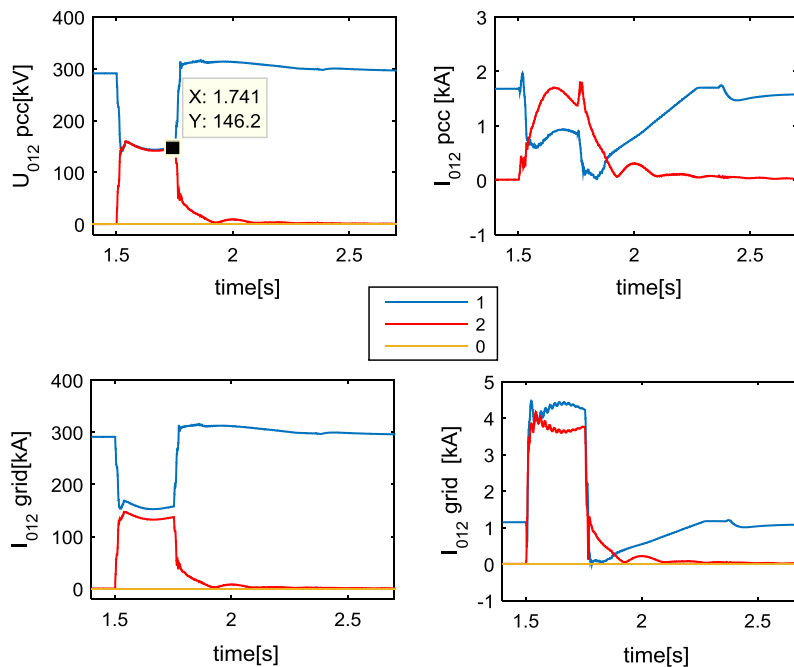


**Fig. 20.** Response of the GSVSC during balanced fault for case 4. Upper subplots show the sequence voltages and currents at the PCC while lower subplots at the infinite grid.

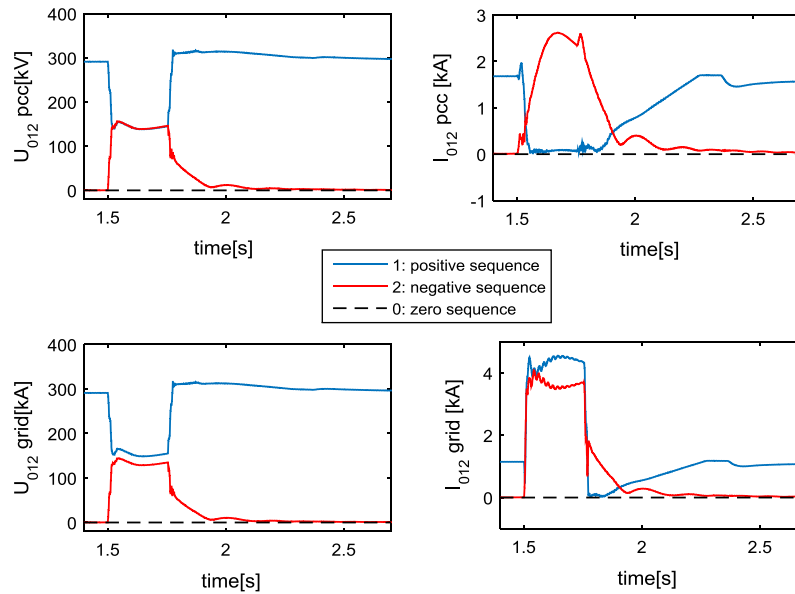


**Fig. 21.** Response of the GSVSC during balanced fault for case 5. Upper subplots show the sequence voltages and currents at the PCC while lower subplots at the infinite grid.

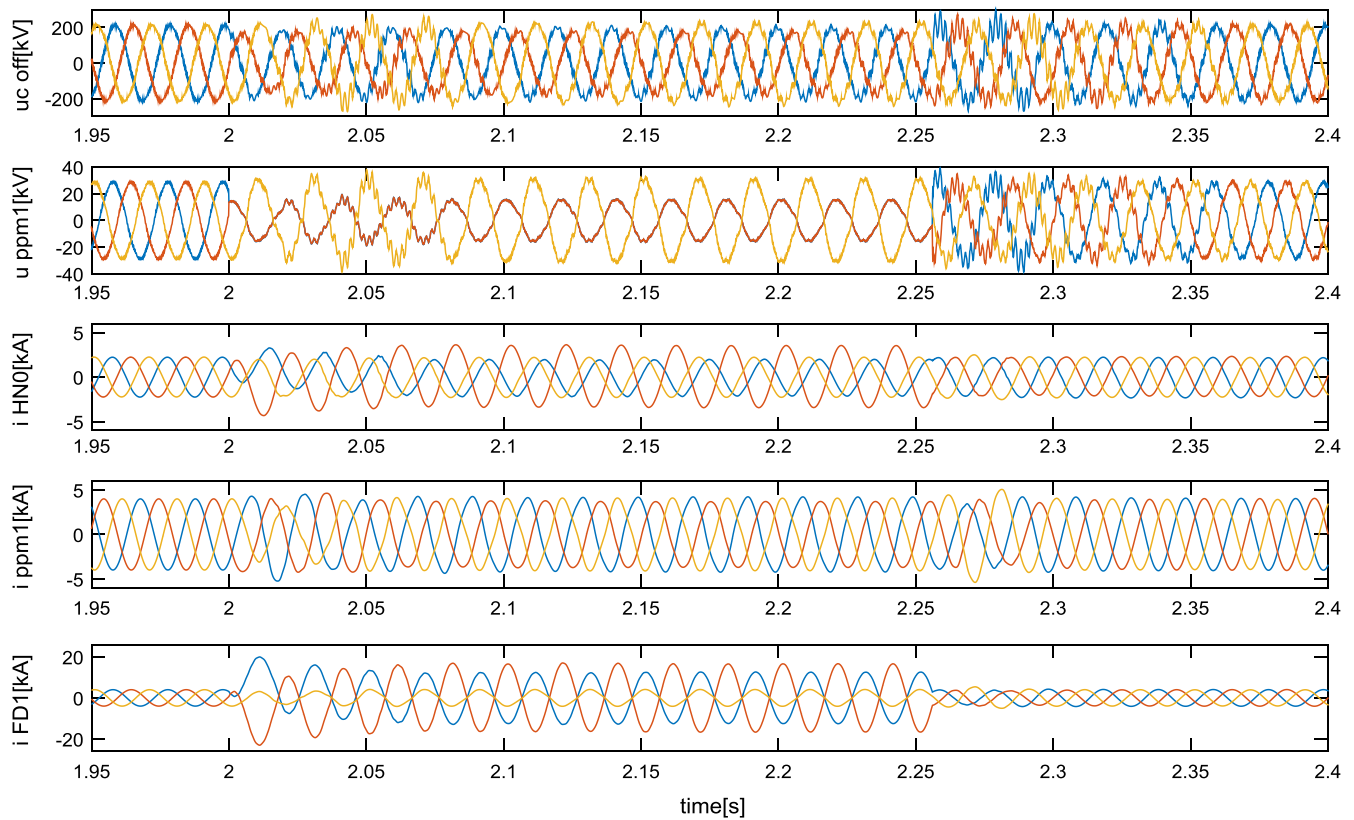


**Fig. 22.** Response of the offshore AC island to a line-to-line fault in the PPM1 terminals. From top to bottom, the instantaneous voltage at the wind park VSC (WPVSC) HVDC converter terminal, the instantaneous voltage at PPM1 terminal, the current at WPVSC terminal, the current at the PPM1 and the current at the FD1, 33 kV point. The simulation is for case 1 of Section 6.3.

seen in Fig. 23. The wind turbines before the fault operate with maximum power generation (with rated current 4 kA per each PPM). As it can be observed in Figs. 22 and 23, the fault current injection of the wind turbine lies in the steady state region. In addition, an adequate fault current level is measured at the FD1 point, where the breaker is installed.

### 6.3.2. Case 2: Line-to-line fault case with negative sequence current suppression and $k1 = 0$ (with the FRT reduction method)

Here, the proposed positive-sequence-voltage-dependent (PSVD) active current reduction at the offshore wind turbines is assumed to be in operation. The presented results aim to demonstrate that the PSVD loop in Fig. 9 does not jeopardize the fault

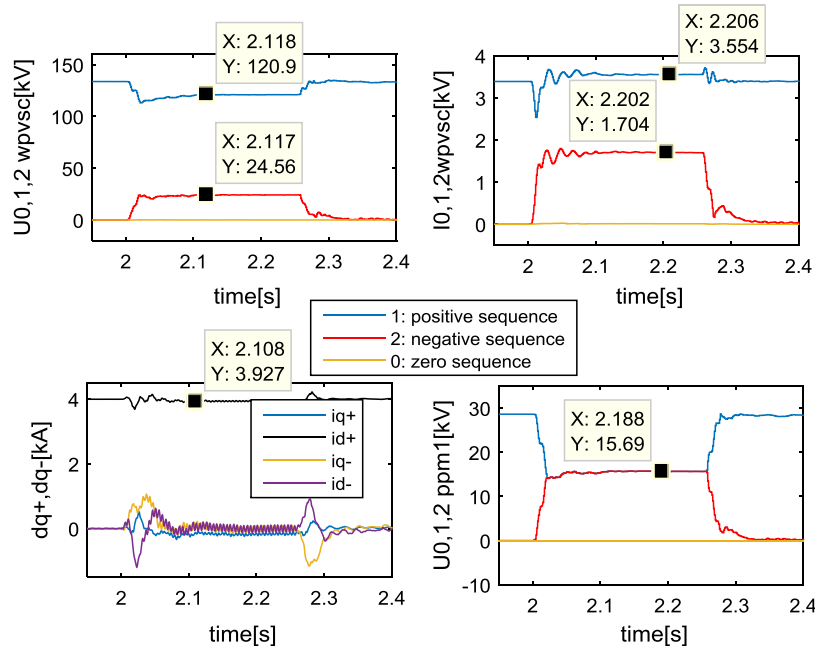


**Fig. 23.** Response of the offshore AC island to a line-to-line fault in the PPM1 terminals. Upper subfigures: the sequence components of WPVSC terminal. Lower subfigures: the dq-positive, the dq-negative sequence currents of the PPM1, and the sequence voltages at the PPM1 terminal. The simulation is for case 1 of Section 6.3.

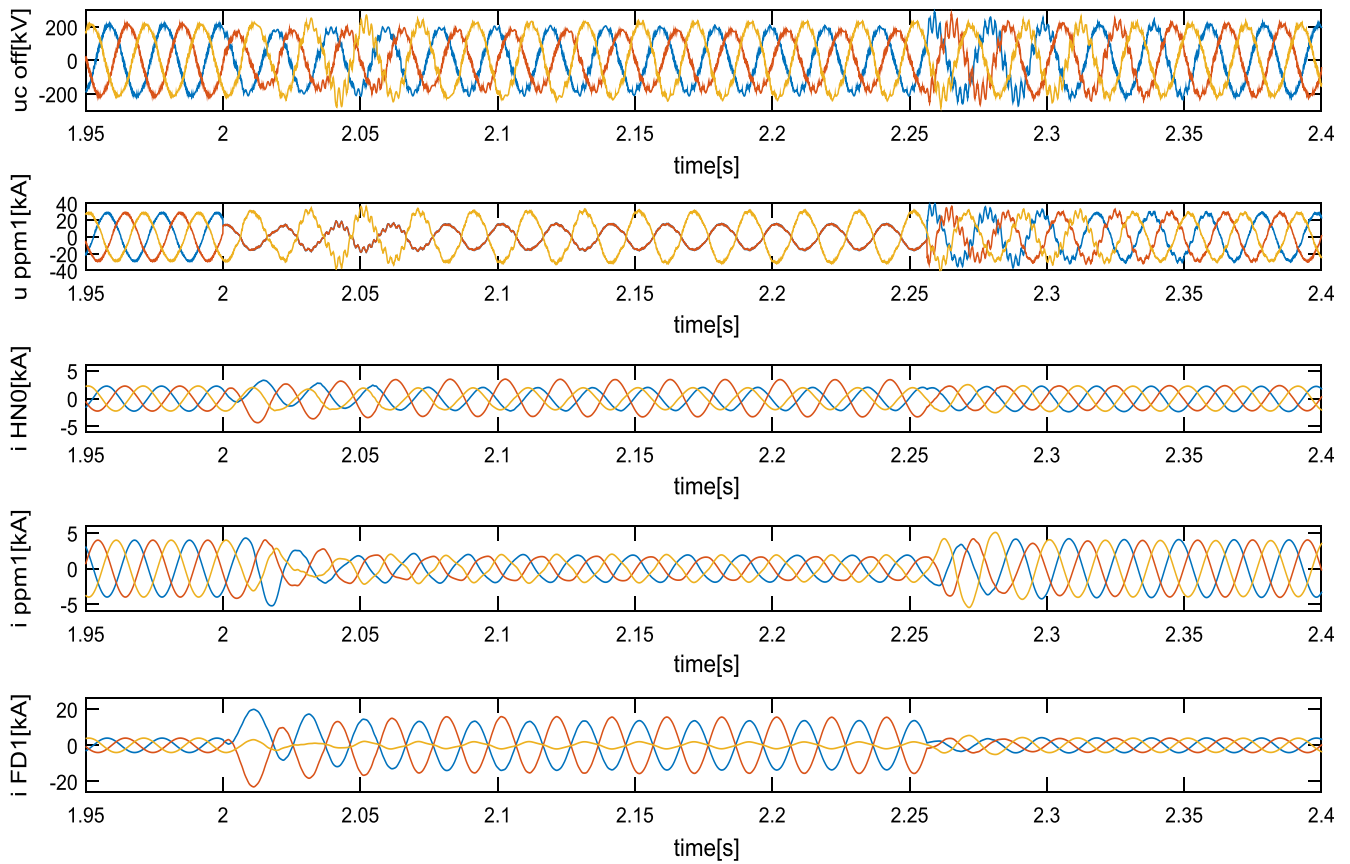


**Fig. 24.** Response of the offshore AC island to a line-to-line fault in the PPM1 terminals. From top to bottom, the instantaneous voltage at the wind park VSC (WPVSC) HVDC converter terminal, the instantaneous voltage at PPM1, the current at WPVSC, the current at the PPM1 and the current at the FD1 point. Simulation is for case 2 of Section 6.3.

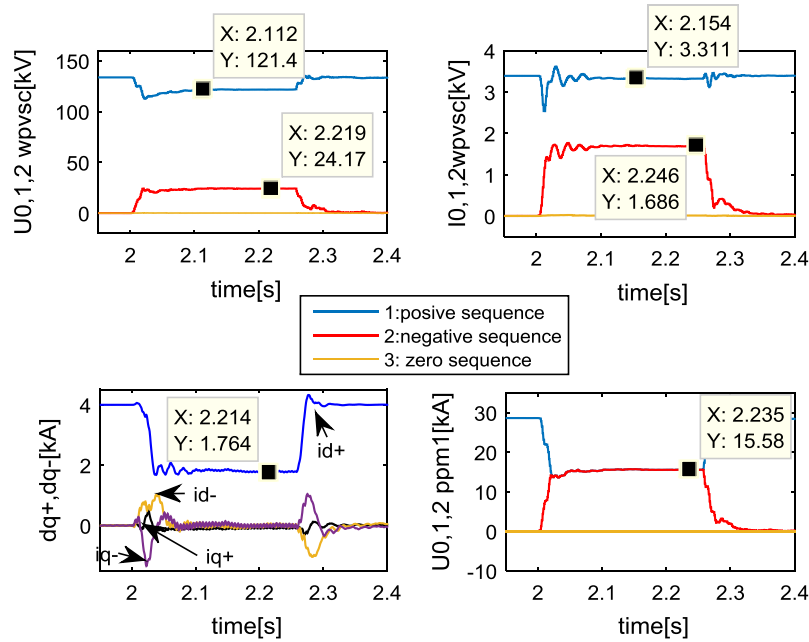


**Fig. 25.** Response of the offshore AC island to a line-to-line fault in the PPM1 terminals. Up the sequence components of WPVSC terminal, down, the dq-positive and dq-negative sequence currents of the PPM1, and the sequence voltages at the PPM1 terminal. Simulation is for case 2 of Section 6.3.

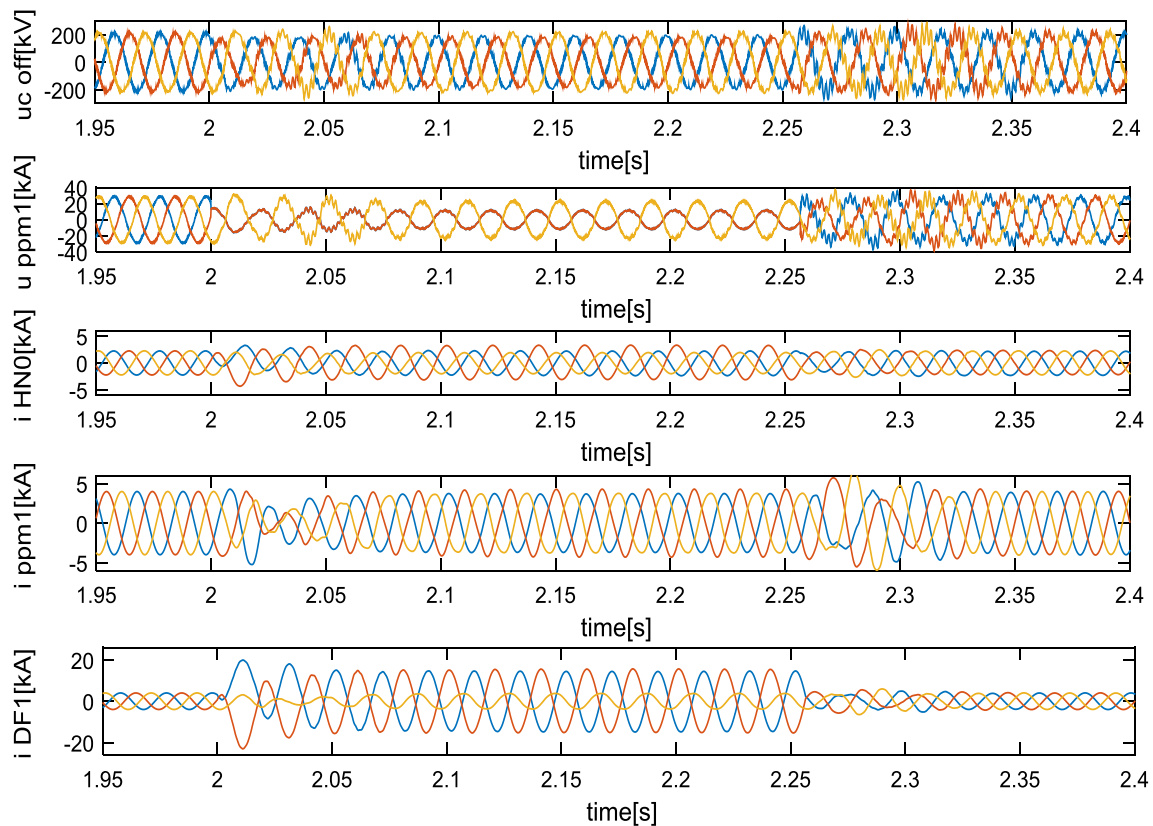


**Fig. 26.** Response of the offshore AC island to a line-to-line fault in the PPM1 terminals. From top to bottom, the instantaneous voltage at the wind park VSC (WPVSC) HVDC converter terminal, the instantaneous voltage at PPM1, the current at WPVSC, the current at the PPM1 and the current at the FD1 point. Simulation is for case 3 of Section 6.3.

detection capability of the island grid and does not reduce the offshore island fault currents, at least at the FD1 point where the fault needs to be cleared. Similar to the previous case, no reactive current injection is performed during the unbalanced fault period.

As it can be observed in Figs. 24 and 25, the total fault current injection from the offshore PPM1 is smaller in this case given that neither reactive positive sequence current is provided nor negative sequence current (see Fig. 25). Observing the fault current mea-

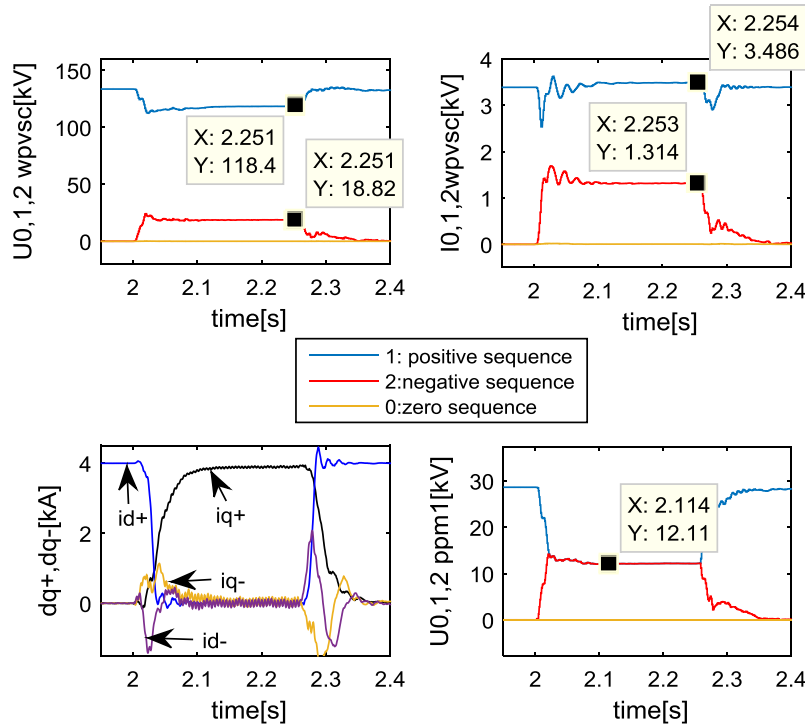


**Fig. 27.** Response of the offshore AC island to a line-to-line fault in the PPM1 terminals. Up the sequence components of WPVSC terminal, down, the dq-positive and dq-negative sequence current of the PPM1, and the sequence voltages at the PPM1 terminal. Simulation is for case 3 of Section 6.3.

sured at FD1, it can be seen that the use of the proposed in this work FRT module for the FRT enhancement of the HVDC link, does not affect the fault detection capability in the island grid. The fault current level at the FD1 is at the same value as in the previous case where the active current is not reduced. Furthermore, not much difference is observed compared to the base case 1, with regard to the positive and the negative sequence voltage profiles of the offshore island grid. From these results, it can be seen that under unbalanced faults the operation of the proposed enhanced FRT scheme for the HVDC link does not jeopardize neither the operation of the protection schemes nor the voltage profiles during the fault period.

### 6.3.3. Case 3: Line-to-line fault with negative sequence current suppression and positive sequence reactive current injection

So far, it has been assumed that no positive sequence current is provided to the offshore AC island. This paragraph addresses the effect of the reactive current injection during line-to-line faults on the unbalanced fault response of the offshore island AC grid. In that prospect, Figs. 26 and 27 present the line-to-line fault case, where the wind turbines suppress the negative sequence current and inject only positive sequence reactive current proportionally to the positive sequence voltage.

As it can be seen in Figs. 26 and 27, the PPM1 fault current injection is symmetrical since only positive sequence is provided. The active current in the wind turbines is reduced to zero, because all the fault current capacity is provided as reactive current. The positive and the negative sequence voltage at the PPM1 is presented in Fig. 27. Compared to the case 2, in this case it can be seen that the reactive positive sequence current injection leads to lower positive sequence voltage levels at the PPM1. Hence, during unbalanced faults, the reactive positive sequence current injection for the power electronic based offshore island does not bring the expected benefits in the offshore system concerning the voltage support. In that prospect, reactive current injection during unbal-

anced faults in the offshore island grid can be avoided since the offshore HVDC station provides adequate fault current levels in the 33 kV.

## 7. Conclusion

In this paper the FRT response of offshore wind power plants with VSC-HVDC transmission is assessed for onshore and offshore AC faults. An enhanced voltage drop FRT control strategy is proposed. The use of the positive-sequence-voltage-dependent (PSVD) active current reduction control module at the offshore wind turbines, ensures improved FRT compliance for the HVDC link. Although during offshore AC faults the application of the active current reduction at the offshore wind turbines reduces their fault current injections, it does not affect significantly the fault current levels at the 33 kV feeder.

In addition, the paper investigates on the unbalanced fault response of the VSC-HVDC link during onshore transmission system faults. It is demonstrated that the suppression of the negative sequence reactive current by the onshore HVDC converter station leads to steady state value fault current levels. The latter depends on the operating point and does not always utilize all the fault current capacity of the HVDC converter station. In that context, fault detection problems might arise in future power systems with large amount of power electronic interfaced generation and transmission units, where the short circuit currents levels are reduced. In that frame, a variety of control strategies are tested for the onshore VSC-HVDC station. It is presented that due to the limited fault-current capacity of the onshore HVDC station, the combined positive and negative sequence reactive current injection is not achievable when reactive positive sequence currents are provided during unbalanced faults. With purpose to solve this bottleneck, a new control module is proposed which reduces the positive sequence active current during unbalanced faults proportionally to the negative sequence voltage. In this way, negative sequence currents can



be provided in order to enhance the protection of the AC transmission lines where VSC-HVDC systems are connected.

## References

- [1] Song HS, Nam K. Dual current control scheme for PWM converter under unbalanced input voltage conditions. *IEEE Trans Ind Electron* 1999;46(5):953–9.
- [2] Yazdani A, Iravani R. A unified dynamic model and control for the voltage-sourced converter under unbalanced grid conditions. *IEEE Trans Power Deliv* 2006;21(3):1620–9.
- [3] Ma KL, Chen W, Liserre M, Blaabjerg F. Power controllability of a three-phase converter with an unbalanced ac source. *IEEE Trans Power Electron* 2015;30(3):1591–604.
- [4] Ng C, Ran L, Bumby J. Unbalanced grid fault ride-through control for a wind turbine inverter. In: Industry applications conference, 2007, 42nd IAS annual meeting, conference record of the 2007 IEEE 2007 Sep 23. IEEE; 2007. p. 154–64.
- [5] Engelhardt S, Kretschmann J, Fortmann J, Shewarega F, Erlich I, Feltes C. Negative sequence control of DFG based wind turbines. In: Power and energy society general meeting, 2011 IEEE 2011 Jul 24. IEEE; 2011. p. 1–8.
- [6] Neumann T, Wijnhoven T, Deconinck G, Erlich I. Enhanced dynamic voltage control of type 4 wind turbines during unbalanced grid faults. *IEEE Trans Energy Convers* 2015;30(4):1650–9.
- [7] Erlich I, Feltes C, Shewarega F. Enhanced voltage drop control by VSC–HVDC systems for improving wind farm fault ride through capability. *IEEE Trans Power Deliv* 2014;29(1):378–85.
- [8] Xu L, Andersen BR, Cartwright P. VSC transmission operating under unbalanced AC conditions-analysis and control design. *IEEE Trans Power Deliv* 2005;20(1):427–34.
- [9] Chaudhary SK, Teodorescu R, Rodriguez P, Kjaer PC, Gole AM. Negative sequence current control in wind power plants with VSC-HVDC connection. *IEEE Trans Sustain Energy* 2012;3(3):535–44.
- [10] Moawwad A, Moursi E, Shawky M, Xiao W. A novel transient control strategy for VSC-HVDC connecting offshore wind power plant. *IEEE Trans Sustain Energy* 2014;5(4):1056–69.
- [11] ENTSO-E. Draft network code on high voltage direct current connections and dc connected power park modules. Brussels; April 2014. <https://www.entsoe.eu/major-projects/network-code-development/high-voltage-direct-current/Pages/default.aspx>.
- [12] Xu L, Yao L, Sasse C. Grid integration of large DFIG-based wind farms using VSC transmission. *IEEE Trans Power Syst* 2007;22(3):976–84.
- [13] Feltes C, Wrede H, Koch FW, Erlich I. Enhanced fault ride-through method for wind farms connected to the grid through VSC-based HVDC transmission. *IEEE Trans Power Syst* 2009;24(3):1537–46.
- [14] van der Meer A, Ndreko M, Gibescu M, van der Meijden M. The effect of FRT behavior of VSC-HVDC-connected offshore wind power plants on AC/DC system dynamics. *IEEE Trans Power Deliv* 2016;31(2):878–87.
- [15] Nanou SI, Patsakis GN, Papathanassiou SA. Assessment of communication-independent grid code compatibility solutions for VSC–HVDC connected offshore wind farms. *Electr Power Syst Res* 2015;30(121):38–51.
- [16] Mitra P, Zhang L, Harnefors L. Offshore wind integration to a weak grid by VSC-HVDC links using power-synchronization control: a case study. *IEEE Trans Power Deliv* 2014;29(1):453–61.
- [17] Saeedifard M, Iravani R. Dynamic performance of a modular multilevel back-to-back HVDC system. *IEEE Trans Power Deliv* 2010;25(4):2903–12.
- [18] Moon JW, Park JW, Kang DW, Kim JM. A control method of HVDC-modular multilevel converter based on arm current under the unbalanced voltage condition. *IEEE Trans Power Deliv* 2015;30(2):529–36.
- [19] Tu Q, Xu Z, Chang Y, Guan L. Suppressing DC voltage ripples of MMC-HVDC under unbalanced grid conditions. *IEEE Trans Power Deliv* 2012;27(3):1332–8.
- [20] Guan M, Xu Z. Modeling and control of a modular multilevel converter-based HVDC system under unbalanced grid conditions. *IEEE Trans Power Electron* 2012;27(12):4858–67.
- [21] Li Shaohua, Wang Xiuli. Circulating current suppressing strategy for MMC-HVDC based on non-ideal proportional resonant controllers under unbalanced grid conditions. *IEEE Trans Power Electron* 2015;30(1):387–97.